

# Distributed Stochastic Gradient Descent with Staleness: A Stochastic Delay Differential Equation Based Framework

Siyuan Yu, Wei Chen, *Senior Member, IEEE*, and H. Vincent Poor, *Life Fellow, IEEE*

**Abstract**—Distributed stochastic gradient descent (SGD) has attracted considerable recent attention due to its potential for scaling computational resources, reducing training time, and helping protect user privacy in machine learning. However, the staggers and limited bandwidth may induce random computational/communication delays, thereby severely hindering the learning process. Therefore, how to accelerate asynchronous SGD by efficiently scheduling multiple workers is an important issue. In this paper, a unified framework is presented to analyze and optimize the convergence of asynchronous SGD based on stochastic delay differential equations (SDDEs) and the Poisson approximation of aggregated gradient arrivals. In particular, we present the run time and staleness of distributed SGD without a memorylessness assumption on the computation times. Given the learning rate, we reveal the relevant SDDE's damping coefficient and its delay statistics, as functions of the number of activated clients, staleness threshold, the eigenvalues of the Hessian matrix of the objective function, and the overall computational/communication delay. The formulated SDDE allows us to present both the distributed SGD's convergence condition and speed by calculating its characteristic roots, thereby optimizing the scheduling policies for asynchronous/event-triggered SGD. It is interestingly shown that increasing the number of activated workers does not necessarily accelerate distributed SGD due to staleness. Moreover, a small degree of staleness does not necessarily slow down the convergence, while a large degree of staleness will result in the divergence of distributed SGD. Numerical results demonstrate the potential of our SDDE framework, even in complex learning tasks with non-convex objective functions.

**Index Terms**—Distributed optimization, machine learning, stochastic gradient descent, gradient staleness, computational delay, communication bandwidth, stochastic delay differential equations, asynchronous algorithm, event-based signal processing, performance analysis

## I. INTRODUCTION

Deep neural networks (DNNs) have found widespread applications in diverse fields, including computer vision, natural language processing, and emerging areas like textual data analysis [1], in which high-performance multi-GPU computing is enabled by GPU-oriented interconnects such as NVLink [2]. Computer networks, supported by communication protocols [3], [4], often serves as the interconnecting infrastructure enabling efficient resource sharing among network nodes [5], which provides the essential framework for distributed AI systems to communicate and access resources. Stochastic gradient descent (SGD) serves as the fundamental framework for most existing deep learning algorithms, enabling models to learn from extensive databases and attain exceptional performance.

Although parallelizing training can accelerate the training process, the presence of straggling workers can lead to idle time, reducing the speedup potential. In traditional synchronous learning, faster devices are forced to wait for slower

ones due to the heterogeneity of the devices. To tackle this issue, asynchronous learning has been proposed, where each worker pushes gradients to the server in an event-triggered manner [7]–[13]. As an important advantage of asynchronous SGD, it has been shown to achieve better performance compared to synchronous SGD with respect to wall-clock time [14]. Though asynchronous SGD eliminates waiting overhead, it suffers from higher convergence errors due to gradient staleness, which is induced by the computational delay and communication delay [15], [17]. As a result, stale gradients are usually penalized using a staleness-dependent learning rate in staleness-aware asynchronous SGD [18]–[21]. Also, the communication load can be reduced in distributed learning via event-triggered communication, referred to as event-triggered stochastic gradient descent [22]–[26].

For the theoretical convergence analysis of SGD, classical bound-type results include [27] and [28]. Existing bound-type results for SGD with stale-gradient include [14], [16], [29], [30], [32], [33]. The key obstacle to deal with in asynchronous learning is gradient staleness. In [29], asynchronous SGD is shown to suffer an asymptotic penalty in convergence rate due to gradient staleness. In the presence of gradient delays, Agarwal and Duchi demonstrate that asynchronous learning can achieve order-optimal convergence results in [30]. As is also presented in [32], asynchronous SGD achieves similar convergence property as the centralized counterpart with bounded communication delay. To tackle this issue of gradient staleness, by carefully tuning the algorithm's step size, asynchronous learning is shown to still converge the critical set in [34]. In addition to the classical bound type analysis, performance analysis based on continuous approximation by stochastic differential equation also attracted considerable attention in stochastic approximation literature [35], [36]. In [38], the author uses tools from stochastic calculus and asymptotic analysis to provide a precise dynamical description of SGD and its variants, based on which adaptive learning rate policies are presented. In [37], the authors approximated SGD in terms of a multivariate Ornstein-Uhlenbeck process, where precise, albeit only distributional, descriptions of the SGD dynamics are presented in complement to the classical bound type converge analysis. In addition, the authors conduct theoretical analysis on the convergence rates through the continuous approximation by stochastic differential delay equations in [33].

To provide non-asymptotic performance analysis and gain greater insights into the impact of gradient staleness on the convergence of distributed SGD, in this paper, a stochastic approximation-based approach is presented, in complement to the conventional bound type analysis. Similar to [10], [37], [38], we first focus on quadratic objective functions and then extend our discussion to general cases. Further, we aim to derive criteria for the parameter setup of learning rates, the total number of workers, and communication protocol in asynchronous distributed learning with gradient staleness. In the literature, closely related works are [14], [15] in terms of

This research was supported in part by the NSFC/RGC Joint Research Scheme under Grant No. 62261160390, and in part by U.S National Science Foundation under Grant ECCS-2335876. An earlier version of this paper is to be presented in part at the 2024 IEEE International Conference on Communications (ICC) [6].

wall-clock run-time analysis, [37], [38] in terms of stochastic differential equation approximation, and [33] in terms of the connection between asynchronous SGD and stochastic delay differential equations (SDDEs). In this work, we aim to extend the run-time analysis for the variants of SGD with exponential processing times [14] to non-memoryless cases, and stochastic differential equation approximation for SGD in [37], [38] to SDDE approximation for asynchronous SGD with gradient staleness. In this work, in complement to the conventional bound-type analysis, we aim to present an SDDE-based approach to reveal the convergence rate of asynchronous SGD. In addition, the run-time and step staleness analysis is further presented. Specifically, the contribution of this paper can be summarized as follows:

- We present a unified framework to analyze and optimize the convergence process of asynchronous SGD with gradient noise and staleness based on SDDEs. To deal with the non-exponentially distributed computation time, a Poisson approximation for the superposition of independent renewal processes is adopted, based on which we present the probability distribution of the update interval and the step staleness or discrete-time gradient staleness of asynchronous SGD. Based on the runtime and staleness analysis, we bridge the behavior of the asynchronous SGD algorithm and the solutions of the SDDE. In particular, the convergence time or rate of convergence of the SGD algorithm can be determined based on the first hitting time of the stochastic process or characteristic roots of the SDDE. It is interestingly shown that, regardless of the specific distribution of computation time, the expectation of the step staleness in asynchronous SGD without gradient dropout is only determined by the number of workers and the group size.
- The performance of the SGD algorithm with stale gradient is demonstrated to be closely related to the product of the step staleness, learning rate, and the 2-norm of the Hessian matrix. Our analysis indicates that a small degree of staleness could slightly accelerate the SGD algorithm, while a large degree staleness could be harmful and result in the divergence of asynchronous SGD. Our analyses align with the observations made by existing literature and complement classical bound-type convergence analyses for SGD with stale gradients. Also, it is shown that the presence of the gradient noise contributes to an increase in the average first hitting time. Under certain circumstances, the increase is proven to be proportional to the standard deviation of the Gaussian noise and the square root of the logarithm of the optimization variable's dimension.
- An excessive number of activated workers does not necessarily accelerate asynchronous SGD. This is due to the fact that a small number of workers provides fewer gradients while a large number of workers leads to a greater degree of staleness. With a staleness-aware learning rate, the positive effect of the increased number of gradients as the number of workers increases can be offset by the staleness-aware step size. The performance of asynchronous SGD with an excess of workers can be improved by selecting an appropriate group size or discarding outdated gradients. The limited bandwidth leads to an increased gradient staleness or a smaller update frequency depending on the client starting the computation of a new gradient right after finishing the computation or the transmission of the old one. In this case, an excessive number of workers can lead to a large communication delay due to network congestion, resulting in a degradation in the performance of SGD. Further, high-resolution quantization of the gradients with large gradient noise can lead to an overload of network

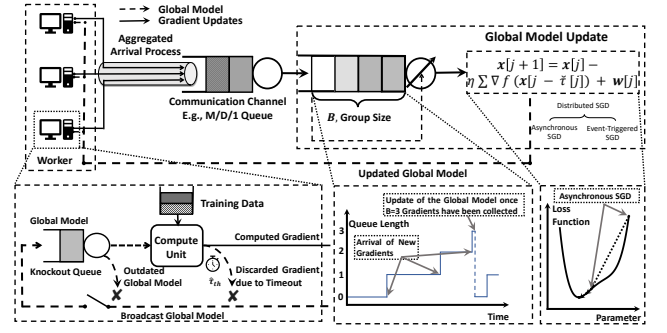


Fig. 1. System model.

bandwidth, thereby being inefficient due to the waste of communication resources.

- A uniformly distributed gradient staleness arises in event-triggered SGD. To characterize the convergence rate of event-triggered SGD, the characteristic roots of the SDDE with uniformly distributed staleness are revealed. Similar to asynchronous SGD, it is shown that a small triggering threshold in event-triggered SGD could slightly accelerate event-triggered SGD and reduce the communication load, while a large triggering threshold may lead to a large degree of staleness and therefore lead to the divergence of event-triggered SGD.

The rest of this paper is organized as follows. Section II presents the system model and the problem formulation. Section III presents the performance analysis for SGD with gradient noise and staleness through a stochastic delay differential equation-based approach. Section IV presents the run-time, staleness, and protocol design criteria for distributed SGD. Simulation results are provided in Section V. Finally, conclusions are drawn in Section VI.

## II. SYSTEM MODEL

In this paper, we are interested in centralized distributed learning involving gradient noise and staleness. Specifically, there is a single central parameter server connected with  $K$  parallel clients, or workers, via a communication medium as illustrated in Fig. 1. In the conventional synchronous setting, the global model evolves based on gradients from all the  $K$  workers at each iteration. To mitigate stragglers in synchronous SGD, asynchronous SGD has been introduced. In the asynchronous setup, each worker can operate independently, fetching the global model and updating its computed gradient. Furthermore, to alleviate the communication overload in distributed learning, event-triggered SGD is presented where the worker updates its gradient to the central server until the difference between the previous gradient and the current one exceeds a given triggering threshold. We introduce the implementation details of asynchronous SGD and event-triggered SGD in Subsections II-A and II-B, respectively, and provide corresponding stochastic approximations.

### A. Asynchronous Distributed Optimization

To mitigate stragglers in synchronous distributed learning, asynchronous distributed learning has emerged as an alternative approach. In the asynchronous setting, each worker operates independently of others, fetching the global model and updating its computed gradient asynchronously. The process unfolds as follows: Firstly, a worker first fetches from the central server the most up-to-date parameters of the model to process the current mini-batch. Subsequently, it computes gradients of the loss function with respect to these parameters.

Notation	Description	Notation	Description
$\hat{\mathbf{x}}(t)/\hat{\mathbf{x}}[j]$	The objective variable in continuous/discrete-time	$K$	The number of total workers
$\hat{\tau}$	Gradient delay or continuous-time gradient staleness	$\mathbf{w}$	Gaussian noise
$\check{\tau}$	Step staleness or discrete-time gradient staleness	$\mathbf{B}(t)$	Standard Wiener process
$\tau$	Gradient staleness in SDDE	$S_j$	The time at which the global model is updated
$f(\cdot)$	The objective function	$\eta$	The learning rate or step size
$\nabla f(\cdot)$	The gradient function	$T_\kappa$	The computational delay of the $\kappa$ th client
$N_p(t)$	The aggregated gradient arrival process	$H$	The first hitting time
$\mathbf{V}$	Hessian matrix of the objective function	$N$	The dimension of the objective function
$v$	The eigenvalues of $\mathbf{V}$	$\lambda$	The characteristic roots of the SDDE
$W_k(\cdot)$	The Lambert W function	$\varpi$	A constant number
$\delta$	A small positive number	$\mu_Q$	The service rate of the bandwidth-limited channel
$\nu$	The intensity of the arrival process	$B$	The group size

TABLE I: Table for Notations.

These gradients are then sent to the central server, which then updates the model accordingly. Simultaneously, upon completing the computation, it fetches the updated global model right away, based on which it computes new gradients.<sup>1</sup> In the asynchronous setup, in the asynchronous setup, the gradient utilized to update the global model is often computed based on outdated parameters, leading to gradient staleness, which can impede the convergence of asynchronous SGD. To address this challenge, we explore the following two methods aimed at reducing gradient staleness in asynchronous SGD.

First, in  $B$ -ASGD, the central server updates the global model once  $B$  gradients are collected since the last update, while the workers who fail to update the gradient in the current iteration can continue their computation. In this context,  $B$  is referred to as the group size. In particular, the  $B$  clients, based on whose gradients the global model updates, start the computation of a new gradient based on the updated global model, to reduce the gradient staleness. Note that the  $B$  clients could also start their computation of new gradients right after their gradients are received by the central server. In this case, the asynchronous SGD algorithm is termed  $B$ -batch-ASGD. In this paper, we generally focus on  $B$ -ASGD unless otherwise stated. Note that asynchronous SGD reduces to synchronous SGD if  $B = K$ .

Second, the workers could drop the current computing gradient to avoid a large degree of gradient staleness. In particular, let  $\hat{\tau}_{th}$  denote the continuous-time gradient staleness threshold. More specifically, during the computation of a gradient, if the time since a worker last fetched the global model exceeds  $\hat{\tau}_{th}$ , the worker stops the computation of the current gradient, fetches the current model, and start the computation of a new gradient. In fact, the worker can also drop outdated gradients according to discrete-time staleness or step staleness. In particular, if the number of updates taken by the central server exceeds a pre-given threshold  $\check{\tau}_{th}$  since the client last fetches the global model, the client halts the current training and starts the computation of the new gradient based on the current global model. By this means, asynchronous SGD reduces the gradient delay at the expense of a smaller update frequency. In this context, we call it pure asynchronous SGD when  $B = 1$  and  $\hat{\tau}_{th} = \infty$  or  $\check{\tau}_{th} = \infty$ , also referred to as 1-ASGD without gradient dropout.

In the following, we present the continuous-time update rule for asynchronous SGD. Let  $\mathcal{K}(t)$  be the set of workers

whose gradients arrive at the parameter server until time  $t$  since the global model is last updated. In  $B$ -ASGD, it holds that  $\mathcal{K}(t^+) = \Phi$  if  $\|\mathcal{K}(t)\| = B$ , in which  $t^+$  means a time that is infinitesimally but noticeably later than the time  $t$ . In this context,  $\mathbb{1}\{\|\mathcal{K}(t)\| = B\}$  is 1 at the time that the central server collects  $B$  gradients and updates the global model and 0 otherwise, in which  $\mathbb{1}\{\cdot\}$  denotes the indicator function and  $\|\cdot\|$  denotes the cardinality of a set. Let  $\hat{\mathbf{x}}(\cdot) \in \mathbb{R}^N$  denote the model parameter with respect to the wall-clock time, where the wall-clock time refers to the actual time elapsed and  $N$  is the dimension of the parameter. In this way, the update rule for asynchronous SGD with respect to the wall-clock time is given by

$$\hat{\mathbf{x}}(t^+) = \hat{\mathbf{x}}(t) - \sum_{\kappa \in \mathcal{K}(t)} \eta [\nabla f(\hat{\mathbf{x}}(t - \hat{\tau}^\kappa(t))) + \mathbf{w}^\kappa(t)] \times \mathbb{1}\{\|\mathcal{K}(t)\| = B\}, \quad (1)$$

in which  $\eta$  is the learning rate,  $f(\cdot)$  is the objective function,  $\nabla f(\cdot)$  is the gradient function of the objective function,  $\mathbf{w}^\kappa(\cdot)$  is the gradient noise corresponds to Worker  $\kappa$ 's gradient, and  $\hat{\tau}(\cdot)$  is the gradient delay or the continuous-time gradient staleness. More specifically,  $\eta$  is a constant with a fixed learning rate or a function of the gradient delay or the step staleness with a staleness-aware learning rate. In addition,  $\hat{\tau}(\cdot)$  refers to the time between a worker fetches the global model and updates the computed gradient to the central server and  $\hat{\tau}^\kappa(t)$  denotes the gradient delay of Worker  $\kappa$ 's gradient that is delivered to the central server at time  $t$ . In practice, the gradient delay is joint determined by the computation/communication resources, the group size  $B$ , and the continuous-time or discrete-time staleness threshold  $\hat{\tau}_{th}$  or  $\check{\tau}_{th}$ . Also,  $\mathbf{w}^\kappa(\cdot)$  is determined by the mini-batch size of each client. Here, we adopt the general assumption of the Gaussianity of the gradient noise, which arises from the central limit theorem [41]. Also, we assume that the Gaussian distribution is isotropic and the variances of the gradient noise across each worker are identical.

Next, we aim to bridge the update rule of asynchronous learning in continuous-time (1) and its discrete-time counterpart. Let  $0 = S_0 < S_1 < S_2 < \dots < S_{J^*}$  denote the times at which the central parameter updates the global model, in which SGD meets its stopping criteria after  $J^*$  iterations. In this setting, the discrete-time counterpart of  $\hat{\mathbf{x}}(S_j)$  is denoted by  $\hat{\mathbf{x}}[j]$ . More specifically, it holds that  $J^* = \min_j \{j \in \mathbb{N}^+, \|\hat{\mathbf{x}}[j] - \mathbf{x}^*\| < \delta\}$ , where  $\mathbf{x}^*$  is the optimal solution of the SGD algorithm and  $\delta > 0$  is a pre-given threshold. In literature, the probability distribution of the update interval, denoted by  $I_j = S_j - S_{j-1}$ , is presented under the assumption of exponentially distributed computational

<sup>1</sup>In this paper, we assume that the downlink communication cost is negligible. Also, the time it takes for the central server to update the global model is also assumed to be negligible since the update is based on computed gradients. In this way, each worker could fetch the updated global model and start the computation of a new gradient once it finishes the computation of the old one.



time [14]. Herein, we will characterize the distribution of the update interval  $I$  through a Poisson approximation with non-memoryless computational delay in Subsection IV-A. Let  $N_a(t) = \{\max i | S_i \leq t\}$  and  $N_a(t_1, t_2) = N_a(t_2) - N_a(t_1)$  iterations. More specifically,  $N_a(t)$  is the number of global updates taken before time  $t$ . In this paper, the wall-clock time refers to the actual time elapsed regarding the training process, and the discrete-time counterpart of which is termed iteration or epoch. Clearly, the wall-clock time corresponding to the  $j$ th update of the global model is  $S_j$ . Correspondingly,  $\mathbf{w}^\kappa[\cdot]$  indexes the discrete-time gradient noise of Client  $\kappa$ . Also,  $\|\mathcal{K}(S_j)\| = B$ . Let  $\mathcal{K}[j] = \mathcal{K}(S_j)$  be the set of clients that triggers the  $j$ th update of the global model. Thereby, the update rule of asynchronous learning in discrete-time corresponding to (1) is given by

$$\check{\mathbf{x}}[j+1] = \check{\mathbf{x}}[j] - \sum_{\kappa \in \mathcal{K}[j]} \eta (\nabla f(\check{\mathbf{x}}[j - \check{\tau}_B^\kappa[j]]) + \mathbf{w}^\kappa[j]), \quad (2)$$

in which  $\check{\tau}_B^\kappa[j]$  is the iterations taken by the global model between Worker  $\kappa$  fetches the global model and finishes the computation of the gradient that contributes to the  $j$ th update of the global model. In  $B$ -ASGD, the relationship between the step staleness or discrete-time staleness  $\check{\tau}^\kappa[j]$  and  $\check{\tau}_B^\kappa[j]$  is given by  $\check{\tau}^\kappa[j] = \check{\tau}_B^\kappa[j] \times B$ , since the global model is updated based on  $B$  gradients at each iteration. The relationship between the discrete-time gradient staleness  $\check{\tau}^\kappa[j]$  and the continuous-time staleness  $\hat{\tau}^\kappa(t)$  in  $B$ -ASGD are given by

$$\check{\tau}^\kappa[j] = N_a(S_j - \hat{\tau}^\kappa(S_j), S_{j-1}) \times B. \quad (3)$$

Let the step staleness of the arrived gradients be denoted by the random variable  $\check{\tau}$ . Intuitively, a larger  $\mathbb{E}\{\check{\tau}\}$  corresponds to an increased training error, as discussed in [18]. Also, it is noteworthy that a larger gradient delay does not necessarily result in a greater step staleness.

Let  $\mathbf{x}(\cdot)$  denote the continuous approximation of  $\hat{\mathbf{x}}(\cdot)$  with respect to the stochastic differential equation. In this way, the continuous approximation for asynchronous SGD is presented via the following stochastic delay differential equation:

$$d\mathbf{x}(t) = -\nabla f(\mathbf{x}(t - \tau(t)))dt + \sigma d\mathbf{B}(t), \quad (4)$$

in which  $\nabla f(\mathbf{x})$  is the gradient of the objective function  $f(\cdot)$  at  $\mathbf{x}$ ,  $\tau(t)$  is the stochastic process characterizing the gradient staleness in the SDDE,  $\mathbf{B}(t)$  or  $B(t)$  is an  $N$ -dimensional or one-dimensional standard Brownian motion or Wiener process, and  $\sigma > 0$  is the standard variance of the Brownian motion.<sup>2</sup>

Let  $\check{\tau}^{(n)}$  denote the step staleness of the  $n$ th gradient that is delivered to the central server. With a fixed learning rate  $\eta$ , the gradient staleness in SDDE is given by  $\tau(t) = \eta\check{\tau}^{(n)}$  for  $t \in ((n-1)\eta, n\eta)$ .<sup>3</sup> The relationship between  $\hat{\mathbf{x}}(\cdot)$  and its continuous-time approximation  $\mathbf{x}(\cdot)$  is  $\hat{\mathbf{x}}(t) \approx \mathbf{x}(\eta N_a(t)B)$ .

### B. Event-Triggered Distributed Optimization

In this subsection, we present the implementation of ET-SGD. In distributed SGD with limited bandwidth, event-triggered SGD can be adopted to effectively reduce bandwidth usage. In particular, different from asynchronous SGD, time is partitioned into fixed-length time slots in the ET-SGD

<sup>2</sup>To be rigorous, given the learning rate  $\eta$  and the standard variance of  $\mathbf{w}[\cdot]$ , denoted by  $\check{\sigma}$ , the relationship between the standard variance of Brownian motion in (4) and the Gaussian noise in (2) is  $\sigma = \frac{1}{\sqrt{\eta}}\check{\sigma}$ .

<sup>3</sup>A careful reader may notice that if the central server performs updates of the global model based on multiple gradients at one time, it could introduce subtle differences in gradient staleness in SDDE, as later-added gradients may suffer a greater staleness. In this paper, we ignore this effect due to its minor impact. Also, the approximation error of (4) is investigated in [33] and is therefore beyond the scope of this paper.

setup. Let  $T_s$  denote the time slot length. The central server performs updates of the model at wall-clock time  $jT_s$  for  $j \in \mathbb{N}^+$ . Further, the communication between the workers and the central server follows an event-triggered manner. In this scheme, each worker communicates its gradient to the server only upon a certain event is triggered. More specifically, the triggering condition is that the difference between the current gradient and the last updated gradient is greater than a pre-given threshold.

In particular, the central server broadcasts the current model to all the workers at each iteration. Based on the received model and the local dataset, each worker computes a gradient. Further, it is assumed that each worker could finish the computation of the gradient within a timeslot. More specifically, the gradient computed by Worker  $\kappa$  at iteration  $j$  is denoted by  $\mathbf{g}^\kappa[j] = \nabla f(\check{\mathbf{x}}[j]) + \mathbf{w}^\kappa[j]$ . Note that the workers skip transmission of the current gradient at the epoch when the current gradient and the last updated gradient do not differ too much [24]. More specifically, the triggering criterion is given by  $\|\mathbf{g}^\kappa[j] - \hat{\mathbf{g}}^\kappa[j^-]\|_2 \geq \xi$  in which  $\mathbf{g}^\kappa[j]$  is the newly computed gradient,  $\hat{\mathbf{g}}^\kappa[j^-]$  is Worker  $\kappa$ 's last updated gradient before time  $j^-$ ,  $\|\cdot\|_2$  denotes the 2-norm, and  $\xi$  is the threshold in event-triggered SGD. Further, let  $\hat{\mathbf{g}}^\kappa[j] = \mathbf{g}^\kappa[j - \check{\tau}^\kappa[j]]$ , in which  $\check{\tau}^\kappa[j]$  is the gradient staleness arises in event-triggered SGD and  $\check{\tau}^\kappa[j] = 0$  if Worker  $\kappa$  update its gradient at time  $j$ . In this way, the update rule of the global model in event-triggered SGD in discrete-time is  $\check{\mathbf{x}}[j+1] = \check{\mathbf{x}}[j] - \frac{\eta}{K} \sum_{\kappa=1}^K \hat{\mathbf{g}}^\kappa[j - \check{\tau}^\kappa[j]]$ . Slightly different from the asynchronous SGD setting, the learning rate is  $\eta/K$  with  $K$  workers in event-triggered SGD. Correspondingly, the update rule of event-triggered SGD can be also be viewed as the discrete-time version of the continuous-time process (4), in which  $\tau(t) = \eta\check{\tau}^\kappa[j]$  for  $t \in ((j-1)\eta + (\kappa-1)\eta/K, (j-1)\eta + \kappa\eta/K)$  and  $\hat{\mathbf{x}}[j] \approx \mathbf{x}(j\eta)$  in event-triggered SGD.

In Section III, we aim to reveal the relationship between gradient staleness and noise and the convergence rate of the SDDE. In Section IV, we shall reveal how the protocol parameters  $K$ ,  $B$ , and the computational/communication delays determine  $N_a(t)$  and the step staleness  $\check{\tau}$ , as well as the gradient dropout schemes that can be adopted to trade update frequency for a smaller step staleness. According to the SDDE approximation, we bridge the convergence rate of asynchronous SGD and the learning rate, the objective function, and the protocol parameters, based on which the protocol design criteria are further revealed.

## III. A UNIFIED FRAMEWORK FOR CONVERGENCE ANALYSIS OF DISTRIBUTED SGD

In this section, we present theoretical performance analyses for the relationship between the gradient staleness and noise and the convergence of distributed SGD through an SDDE-based approach. To obtain analytical results and find more insights, we first focus on the solvable cases, as was done in, e.g., [37], [38]. Here, we assume that the objective function can be locally approximated by a quadratic function [46]–[48]. Specifically, the objective function takes the form  $f(\mathbf{x}) = \frac{1}{2}(\mathbf{x} - \mathbf{x}^*)^T \mathbf{V}(\mathbf{x} - \mathbf{x}^*)$ , in which  $\mathbf{V} \in \mathbb{R}^{N \times N}$  is a positive-definite matrix,  $\mathbf{x} \in \mathbb{R}^N$  is the objective variable,  $\mathbf{x}^* \in \mathbb{R}^N$  is a constants, and  $[\cdot]^T$  denotes transpose.

### A. A Unified Framework Based on SDDE

For the sake of discussion,  $\mathbf{V}$  is assumed to be a diagonal matrix, i.e.,  $\mathbf{V} = \text{diag}(v_1, v_2, \dots, v_N)$  and it is assumed that

$\mathbf{x}^* = \mathbf{0}$  in which  $\mathbf{0}$  is the vector of zeros.<sup>4</sup> With a quadratic objective function, the continuous-time approximation of distributed SGD with gradient staleness (4) can be represented as:

$$d\mathbf{x}(t) = -\mathbf{V}\mathbf{x}(t - \tau(t))dt + \sigma d\mathbf{B}(t), \quad (5)$$

or

$$dx_i(t) = -v_i x_i(t - \tau(t))dt + \sigma dB(t), \quad (6)$$

for  $i = 1, 2, \dots, N$ . When  $\sigma = 0$ , implying that each gradient is computed based on the entire training dataset where the gradient noise is negligible, Eq. (6) reduces to the deterministic differential equation given by  $dx_i(t) = -v_i x_i(t - \tau(t))dt$ . In addition, when  $\tau(t) = 0$ , which corresponds to synchronous SGD, we obtain  $dx_i(t) = -v_i x_i(t)dt + \sigma dB(t)$  which is an Ornstein-Uhlenbeck process, abbreviated as OU-process. Also, it is observed that the OU process with delay (5) along each eigenvector direction is independent, allowing us to first focus on the one-dimensional case (6) then extend our discussion to the multi-dimensional case.

Next, we demonstrate that the impact of the gradient noise and the gradient staleness can be separately considered taking the case that  $\tau$  is a constant as an example.<sup>5</sup> In this case, the analysis of the behavior of SGD can be based on viewing SGD as a discretization of the following associated stochastic delay differential equation, i.e.,

$$\begin{aligned} dx(t) &= -vx(t - \tau)dt + \sigma dB(t), \\ x(t) &= \varphi(t), \quad t \in [-\tau, 0], \end{aligned} \quad (7)$$

in which  $\varphi(t)$  is a given function on  $[-\tau, 0]$ . Consider the following continuous deterministic differential equation corresponding to Eq. (7), i.e.,

$$\begin{aligned} d\tilde{x}(t) &= -v\tilde{x}(t - \tau)dt, \\ \tilde{x}(t) &= \varphi(t), \quad t \in [-\tau, 0]. \end{aligned} \quad (8)$$

Let  $\tilde{x}_d(t)$  denote a solution to Eq. (8). Then, the solution to Eq. (7) can be given by  $x_s(t) = \tilde{x}_d(t) + \sigma \int_0^t x_0(t-s)dB(t)$ , in which  $x_0(t) = \sum_{k=0}^{\lfloor \frac{t}{\tau} \rfloor} \left[ \frac{v^k}{k!} (t - k\tau) \right]$  in which  $t \in (0, \infty)$ .

In addition, we have  $\tilde{x}_d(t) = x_0(t)\varphi(0) + v \int_{-\tau}^0 x_0(t-s-\tau)\varphi(s)ds$ . It can be noticed that the difference between  $x_s(t)$  and  $\tilde{x}_d(t)$  is only given by a Gaussian distributed random variable, the variance of which is joint determined by the gradient staleness  $\tau$  and the standard variance of the Brownian motion  $\sigma$ .

In the following discussions, we shall present performance analyses for the convergence rate of distributed SGD given gradient noise or gradient staleness through the SDDE-based approach.

### B. The Convergence Speed Given Gradient Noise

In this subsection, we derive a relationship between the convergence time and the gradient noise. To gain more insight on the impact of the gradient noise on the convergence time, we investigate the stochastic processes  $dx_i(t) = -v_i x_i(t)dt + \sigma dB(t)$  for  $i = 1, 2, \dots, N$  in this subsection. In this way, the convergence time of SGD can be modeled as a first hitting time of (5) to the  $\delta$ -neighborhood of the global optimum  $\mathbf{x}^*$ , i.e.,

$$H = \inf\{t > 0 : \|\mathbf{x}(t) - \mathbf{x}^*\|_\infty < \delta\}, \quad (9)$$

<sup>4</sup>The assumption that  $\mathbf{V}$  is a diagonal matrix is with loss of generality. In case  $\mathbf{V}$  is not a diagonal matrix, it holds that  $\mathbf{V} = \mathbf{U}\mathbf{\hat{V}}\mathbf{U}^T$  in which  $\mathbf{\hat{V}}$  is a diagonal matrix by eigenvalue decomposition. By defining  $\tilde{\mathbf{x}} = \mathbf{U}^T(\mathbf{x} - \mathbf{x}^*)$ , we have  $f(\tilde{\mathbf{x}}) = \tilde{\mathbf{x}}^T \mathbf{\hat{V}} \tilde{\mathbf{x}}$ . By this means, we focus on the diagonal  $\mathbf{V}$  in the subsequent discussion.

<sup>5</sup>Note that the gradient staleness  $\tau$  in SDDE is approximately a constant the variance of computation delay of each worker is small with a large worker number in asynchronous SGD, as will be demonstrated in Section IV.

in which the  $i$ th element of  $\mathbf{x}^*$  is denoted by  $x_i^*$ . Defining  $H_i = \inf\{t > 0 : |x_i(t) - x_i^*| < \delta\}$  for  $i = 1, 2, \dots, N$ , it holds that  $H = \max_i\{T_i\}$ .<sup>6</sup> To further demonstrate the impact of the gradient noise on the convergence time of SGD, in this subsection, we first introduce the following lemma on the first hitting time according to [50].<sup>7</sup>

**Lemma 1:** The expectation of the first hitting time  $H_L = \inf\{t > 0 : x_1 \leq x(t) \leq x_1 + dx, x(0) = x_0\}$  of the one-dimensional stochastic process  $dx(t) = s(x)dt + \sigma(x)dB(t)$  is  $\mathbb{E}\{H_L\} = \int_{x_0}^{x_1} \frac{1}{s(x)} dx$ , in which  $s(x)$  is the drift velocity. By Lemma 1, it holds that

$$\mathbb{E}\{H_i\} = \frac{1}{v_i} \log \frac{x_{i,0}}{\delta}, \quad (10)$$

in which  $x_{i,0} = x_i(0)$ .

The probability distributions of the first hitting times  $H_i$  are however complex. To shed more light on the probability characteristics of  $H$ , we shall next present an approximation of the probability distribution of  $T_i$ . Since the first moment of  $H_i$  has already been revealed by Eq. (10), we are interested in the second moment of  $T_i$  in the following discussion.

Given an OU process described by Eq. (6),  $x_i(t)$  follows a Gaussian distribution with mean  $\mathbb{E}\{x_i(t)\} = x_{i,0}e^{-v_i t}$  and variance  $\text{Var}\{x_i(t)\} = \frac{\sigma^2}{2v_i} (1 - e^{-2v_i t})$ . The drift velocity at the time that the OU process enters the  $\delta$  neighborhood of the global optimum can be approximated by  $s \approx v_i \delta$  by Eq. (6). By this means, the variance of the first hitting time  $H_i$  can be given by  $\text{Var}\{H_i\} \approx \frac{\sigma^2}{2v_i^3 \delta^2} \left(1 - \frac{1}{\alpha_i^2}\right)$ , in which  $\alpha_i = x_{i,0}/\delta$ . Then, the first hitting time can be approximated as Gaussian distributed as follows:

$$H_i \sim \mathcal{N}\left(\frac{\log \alpha_i}{v_i}, \frac{\sigma^2}{2v_i^3 \delta^2} \left(1 - \frac{1}{\alpha_i^2}\right)\right). \quad (11)$$

Next, we provide further discussion on the probability distribution of  $H = \max_i\{H_i\}$ . Since the first hitting times are approximated Gaussian distributed, we have  $\mathbb{E}\{H\} \approx \mathbb{E}\{H_i\}$  if  $E\{H_i\} \gg E\{H_k\}$  for  $k \neq i$  in which  $i = \arg \max_j E\{H_j\}$ .

Further,  $H_i$  are identically distributed random variable when  $\mathbf{V} = v\mathbf{I}$  and  $\hat{\mathbf{x}}(0) = c\mathbf{1}$ , in which  $v > 0$ ,  $\mathbf{I}$  denotes the identity matrix, and  $\mathbf{1}$  denotes the vector of ones. In this case, we have  $\mathbb{E}\{H_i\} = \frac{1}{v} \log \alpha$  in which  $\alpha = \frac{c}{\delta}$  and  $\text{Var}\{H_i\} \approx \frac{\sigma^2}{2v^3 \delta^2} \left(1 - \frac{1}{\alpha^2}\right)$ . Let

$$\Theta(N) = \mathbb{E}\{\Xi_N\} - \sqrt{\log N}, \quad (12)$$

in which  $\Xi_N = \max\{Z_1, Z_2, \dots, Z_N\}$  and  $Z_i$ s are independent and identically distributed (i.i.d.) standard Gaussian distributed random variable  $Z_i \sim \mathcal{N}(0, 1)$ . More specifically,  $\Xi_N$  is the maximum of  $N$  i.i.d. standard Gaussian random variables. In addition,  $\Theta(N)$  is on the order of  $\mathcal{O}(1)$ . In particular,  $\Theta(1) = 0$ . In this way, it holds that

$$\mathbb{E}\{H\} = \frac{1}{v} \log \alpha + \frac{\sigma \sqrt{1 - \frac{1}{\alpha^2}}}{\sqrt{2v^3 \delta}} \left(\sqrt{\log N} + \Theta(N)\right), \quad (13)$$

in which  $N$  is the dimension of the objective variable  $\mathbf{x}$ .

When  $N = 1$ , it has been shown that the gradient noise does not affect the expectation of the first hitting time in the SGD algorithm by Lemma 1. While Eq. (13) also suggests the same conclusion. Further, the presence of the gradient noise induced an additional term on the average first hitting time,

<sup>6</sup>In this paper, it is generally assumed that the SGD algorithm doesn't leave the  $\delta$ -neighborhood of the global optimum once it enters it when the SGD algorithm converges.

<sup>7</sup>For example, the fact that the expected hitting time of a given level by a standard Brownian motion is infinite is a direct corollary of Lemma 1.

which is proportional to the standard variance of the gradient noise and  $\sqrt{\log N}$  when  $N \geq 2$ .

Next, in order to make the problem analytically tractable and get insightful results, we consider the impact of gradient noise with  $f(\mathbf{x}) = \frac{1}{2}\mathbf{x}^T \mathbf{I} \mathbf{x}$ . Thus, it holds that  $\tilde{\mathbf{x}}[j+1] = \tilde{\mathbf{x}}[j] - \eta \tilde{\mathbf{x}}[j] + \mathbf{w}$ , in which  $\eta$  is the learning rate and  $\mathbf{w}$  is an isotropic Gaussian noise in which  $\mathbf{w} \sim \mathcal{N}(0, \check{\sigma}^2 \mathbf{I})$ . In this case, we define  $\mathbf{r}[j] = \tilde{\mathbf{x}}[j] - \mathbf{x}^*$  and  $r = \|\mathbf{r}\|_2$  to simplify the notations. Due to the symmetric of the normal distribution, the projection of  $\mathbf{w}$  onto the direction of  $\mathbf{r}$ , denoted by  $\mathbf{w}_{\parallel}$ , is also Gaussian distributed, i.e.,  $\|\mathbf{w}_{\parallel}\|_2 \sim \mathcal{N}(0, \check{\sigma}^2)$ . In this context, the component perpendicular to the  $\mathbf{r}$  direction is given by  $\mathbf{w}_{\perp} = \mathbf{w} - \mathbf{w}_{\parallel}$ . In this case, we have  $\langle \mathbf{w}_{\perp}, \mathbf{r} \rangle = 0$ , in which  $\langle \mathbf{a}, \mathbf{b} \rangle$  denotes the inner product of the two vector  $\mathbf{a}$  and  $\mathbf{b}$ . Also, it can be seen that  $\mathbb{E}\{\|\mathbf{w}_{\perp}\|_2^2\} = (N-1)\check{\sigma}^2$ . Thus, it holds that

$$r[j+1] = r[j] - \eta r[j] + \left( \sqrt{r^2[j] + \|\mathbf{w}_{\perp}\|_2^2} - r[j] \right) + w_{\parallel}, \quad (14)$$

in which  $w_{\parallel} = \|\mathbf{w}_{\parallel}\|_2$ . For  $r \gg \check{\sigma}$ , we have  $\sqrt{r^2 + \|\mathbf{w}_{\perp}\|_2^2} - r \approx \frac{\|\mathbf{w}_{\perp}\|_2^2}{2r}$ , since the approximation  $\sqrt{1+s} \approx 1 + \frac{1}{2}s$  holds around the point  $s = 0$ . For a given  $r$ , let the backward speed be defined as  $z = \frac{\|\mathbf{w}_{\perp}\|_2^2}{2r}$ . In this case, it can be seen that the presence of the noise  $\mathbf{w}_{\perp}$  hinders the process of the gradient descent, the speed of which is given by  $z$ . More specifically,  $z$  is Chi-square distributed with mean given by  $\mathbb{E}\{z\} = \frac{(N-1)\check{\sigma}^2}{2r}$ , and variance given by  $\text{Var}\{z\} = \frac{(N-1)\check{\sigma}^4}{r^2}$ . When  $N = 2$ , the backward speed  $z$  follows an exponential distribution. Therefore, the continuous-time approximation of Eq. (14) can be formulated as follows:

$$dr = -\left(\eta r - \frac{(N-1)\check{\sigma}^2}{2r}\right)dt + \sqrt{\sigma^2 + \frac{(N-1)\check{\sigma}^4}{r^2}}dB(t). \quad (15)$$

The first hitting time of the above stochastic process (15) is defined as  $H_d = \inf\{t > 0 : |r(t) - r^*| < \delta, r(0) = r_0\}$ , in which  $r^* = 0$ .<sup>8</sup> By Lemma 1, we obtain the following corollary.

**Corollary 1:** The expectation of the first hitting time  $H_d$  is given by  $\mathbb{E}\{H_d\} = \mathcal{F}(r_0) - \mathcal{F}(\delta)$ , in which  $\mathcal{F}(r) = \frac{1}{2\eta} \log\left(\eta r^2 - \frac{(N-1)\check{\sigma}^2}{2}\right)$ .

*Proof:* According to the primitive function of  $f(r) = \left(\eta r - \frac{(N-1)\check{\sigma}^2}{2r}\right)^{-1}$  with respect to  $r$  and Lemma 1, we arrive at the corollary.  $\square$

In this way, one can notice that the presence of the gradient noise does not affect the expectation of the first hitting time of the gradient descent algorithm when  $N = 1$ . Further, the above analysis also indicates that as the value of  $r$  decreases, the adverse impact of gradient noise on convergence becomes increasingly severe. This also suggests that as the training process progresses, increasing the number of users involved in training or enlarging the mini-batch size to reduce the power of gradient noise could accelerate the convergence of SGD. Note that a high-resolution quantization of the gradients with large gradient noise can lead to a lot of network bandwidth usage, thereby being inefficient due to the waste of communication resources.

<sup>8</sup>Note that the  $H_d$  is defined as the first time that the 2-norm of  $\mathbf{r}$  is smaller than a pre-given threshold. This is different from the definition presented in Eq. (9), which is based on the infinity norm.

### C. The Convergence Speed Given Gradient Staleness

In this subsection, we present an analysis of the SGD with stale through an SDDE-based approach. For the sake of discussion, we shall first focus on the fixed staleness before extending our discussion to the case in which  $\tau$  is a random variable. Let the gradient staleness in SDDE be denoted by a positive constant  $\tau$ . First, we focus on the characteristics of the solution to the deterministic differential equation. By substituting the sampling function  $\varrho(t) = Ae^{\lambda t}$ , in which  $\lambda$  is a complex number into the delay differential equation (8), we have the following characteristics equation:

$$\lambda e^{\lambda \tau} = -v. \quad (16)$$

The function  $h(\lambda) = \lambda e^{\lambda \tau}$  is monotonically decreasing on the interval  $(-\infty, -\frac{1}{\tau})$  and monotonically increasing on the interval  $(-\frac{1}{\tau}, \infty)$ . It has a minimum of  $\inf_{\lambda} h(\lambda) = -\frac{1}{e\tau}$  at  $h(\lambda) = \frac{1}{\tau}$ . Moreover,  $\lim_{\lambda \rightarrow -\infty} h(\lambda) = 0$ .

Therefore, Eq. (16) has a single positive root when  $v < 0$ . In this case, the SGD algorithm with a stale gradient overdamps and does not converge to the global minimum. Further, the characteristic equation has two negative real roots when  $0 < v\tau < \frac{1}{e}$ . In this case, the SGD algorithm with a stale gradient decays monotonically to the global minimum of the quadratic objective function. Moreover, the characteristics equation has a pair of complex conjugate roots with negative real parts when  $\frac{1}{e} < v\tau < \frac{\pi}{2}$ . In this case, the SGD algorithm with stale gradient undergoes damped oscillations. When  $v\tau > \frac{\pi}{2}$ , the real parts of the roots of Eq. (16) becomes positive. Therefore, the SGD algorithm undergoes diverging oscillations. Note that  $\eta$  is the step size of the SGD algorithm. According to the above discussion, we have the following theorem for the discrete-time SGD.

**Theorem 1:** The two roots of the characteristics function Eq. (16) are given by

$$\lambda_k = \frac{W_k(-v\tau)}{\tau}, \quad (17)$$

for  $k = 0, 1$ , in which  $W_k$  is the Lambert W function.

Further, we have the following corollary.

**Corollary 2:** Given the learning rate  $\eta$  and the step staleness  $\check{\tau}$ , the characteristic roots of the continuous-time approximation of the asynchronous SGD algorithm,  $\tilde{\mathbf{x}}[j+1] = \tilde{\mathbf{x}}[j] - \eta v \tilde{\mathbf{x}}[j - \check{\tau}]$ , are given by  $\lambda_k = \frac{W_k(-v\eta\check{\tau})}{\eta\check{\tau}}$  for  $k = 0, 1$ .

For the solvable case, the stochastic gradient descent algorithm with stale gradient converges to the only fixed point when  $\check{\tau} < \frac{\pi}{2\eta v}$ , and without oscillations when  $\check{\tau} < \frac{1}{e\eta v}$ .

With a fixed step size,  $\lambda_k$  are real and negative in which  $|\lambda_0| \leq |\lambda_1|$  when  $\check{\tau} < \frac{1}{e\eta v}$ . Besides, it can be noticed that  $|\lambda_0|$  increases as  $\check{\tau}$  increases for  $\check{\tau} \in (0, \frac{1}{e\eta v})$ . This indicates that the presence of a small degree of gradient staleness accelerates the stochastic gradient descent algorithm, which aligns with the analysis in [14]. However, the SGD algorithm starts to oscillate when  $\check{\tau} \in (\frac{1}{e\eta v}, \frac{\pi}{2\eta v})$ . In addition, the real part of the roots became positive when  $\check{\tau} > \frac{\pi}{2\eta v}$ . It indicates that, the SGD algorithm diverges with a large degree of gradient staleness.

**Remark:** To reveal the characteristic roots of (8) in case  $\tau$  is a random variable, we will present the characteristic roots with uniformly distributed gradient staleness in the forthcoming discussion. Consider Gaussian distributed gradient staleness, i.e.,  $\tau \sim \mathcal{N}(\vartheta, \varsigma^2)$ . Empirically, we find that it holds that



$\lambda_k \approx W_k(-v\vartheta)/\vartheta$  for  $k = 0, 1$  when  $\varsigma \ll \vartheta$ .<sup>9</sup>

Given the gradient staleness, a sensible choice of the learning rate with  $f(x) = \frac{1}{2}vx^2$  is

$$\eta = \frac{1}{ev_N\tilde{\tau}}. \quad (18)$$

For  $f(x) = \frac{1}{2}(x - x^*)^T V(x - x^*)$  in which  $V$  is a diagonal matrix with its diagonal elements given by  $0 \leq v_1 \leq v_2 \leq \dots \leq v_N$ , a sensible choice of the learning rate is given by

$$\eta \in \left( \frac{1}{ev_N\tilde{\tau}}, \frac{\pi}{2v_N\tilde{\tau}} \right). \quad (19)$$

The reason is that if  $\eta \geq \frac{\pi}{2v_N\tilde{\tau}}$ , the SGD algorithm diverges. If  $\eta < \frac{1}{ev_N\tilde{\tau}}$ , the SGD algorithm converges too slow.

**Remark:** Assuming an  $L$ -Lipschitz continuous objective function  $f(x)$ , the step size must be chosen as  $\eta < \frac{\pi}{2L\tilde{\tau}}$  to avoid unbounded oscillations. A more conservative choice  $\eta < \frac{1}{eL\tilde{\tau}}$  ensures that no oscillation occurs. In this case, a small degree of gradient staleness accelerates the SGD algorithm, which aligns with the conclusion in [30], and [31] in which quantization error can be exploited to accelerate the model convergence. Moreover, an appropriate staleness accelerates SGD the convergence in the direction of eigenvectors with small eigenvalues and hinders others with large eigenvalues. The above discussion aligns with the observation made by [14] that a stale gradient may contribute to a faster convergence rate but a higher error floor. In some existing literature [18], [19], the stale-aware step size is inversely proportional to stale, which also aligns with our analysis. However, step size must be carefully chosen with further consideration of the 2-norm of the Hessian matrix of the objective function, to avoid unbounded oscillations.

Next, we proceed with the following discussion on the approximation of the SDDE with a small constant staleness. Recall that we have  $dx(t) = -vx(t-\tau)dt + \sigma dB(t)$ . Further, let  $t_2 = t_1 - \tau$ , and the random variable  $X_{t_2} = x(t_2)$  denote the state value that  $x(t)$  takes at time  $t_2$ . In this way,  $f'(x(t_2)) = vX_{t_2}$ . Additionally,  $X_{t_2}$  is Gaussian distributed given  $x(t_1) = X_{t_1}$  by the definition of an OU process. In this way, it holds that  $\mathbb{E}\{X_{t_2}|x(t_1) = X_{t_1}\} = X_{t_1}e^{v\tau}$ , and  $\text{Var}\{X_{t_2}|x(t_1) = X_{t_1}\} = \frac{\sigma^2}{2}(e^{2v\tau} - 1)$ . Also, it holds that  $\text{Var}\{X_{t_2}|x(t_1) = X_{t_1}\} \approx v\tau\sigma^2$  for  $\tau \ll 1$ . By this means, we conclude that  $X_{t_2} \sim \mathcal{N}(X_{t_1}e^{v\tau}, \frac{\sigma^2}{2}(e^{2v\tau} - 1))$ .

Therefore, we have  $dx(t) = -ve^{v\tau}x(t)dt + \sqrt{\frac{e^{2v\tau}+1}{2}}\sigma dB(t)$ . When  $\tau \ll 1$ , it holds that  $dx(t) = -v(1 + v\tau)x(t)dt + (1 + v\tau/2)\sigma dB(t)$ .

In the following, we present the performance analysis when the gradient staleness is a uniform random variable. In particular, we focus on the uniformly distributed gradient staleness, which can arise in event-triggered SGD. More specifically, consider the delay differential equation given below:

$$dx(t) = -vx(t - \tau(t))dt, \quad (20)$$

in which  $\tau(t_1)$  and  $\tau(t_2)$  are assumed to be identically and independently distributed random variables when  $t_1 \neq t_2$ . Further, it holds that  $\tau(t) \sim U(0, \varsigma)$ . Clearly,  $\mathbb{E}\{\tau\} = \frac{1}{2}\varsigma$ . In the following discussion, we study the first moment of  $\langle x(t) \rangle$ , in which brackets  $\langle \cdot \rangle$  denotes an average over the realizations of the random process  $\{\tau(t)\}$ . In this way, we have the following proposition.

<sup>9</sup>More specifically, we have the following observation of Gaussian distributed gradient staleness through numerical results. When  $\tau \sim \mathcal{N}(\vartheta, \varsigma^2)$  and  $\varsigma \ll \vartheta$ , asynchronous SGD nearly has the same convergence rate as when the gradient staleness is a constant, i.e.,  $\tau = \vartheta$ . With a sufficiently large  $\varsigma$ , asynchronous SGD may diverge despite a small  $\vartheta$ . Analytical results for the staleness of Gaussian distribution gradients are noted as future work.

**Proposition 1:** When the gradient staleness is uniformly distributed, the average  $P(t) = \langle x(t) \rangle$  obeys the second order differential equation given by

$$\frac{d^2P(t)}{dt^2} = -\frac{v}{\varsigma}(P(t) - P(t - \varsigma)). \quad (21)$$

*Proof:* Let  $Q(t) = \int_{t-\varsigma}^t \langle x(s) \rangle ds$ . In this way, it holds that  $\frac{dP(t)}{dt} = -v\frac{Q(t)}{\varsigma}$  and  $\frac{dQ(t)}{dt} = P(t) - P(t - \varsigma)$ . By this means, we arrive at Eq. (21).  $\square$

By Proposition 1, we have the subsequent corollary illustrating the characteristic equation associated with the differential equation given by Eq. (21). Without loss of generality, we assume  $v = 1$  for the sake of discussion in the rest of this subsection.

**Corollary 3:** When  $v = 1$ , the differential equation (21) has the following characteristic equation:

$$\varsigma\lambda^2 = e^{-\varsigma\lambda} - 1. \quad (22)$$

In the following, we present a brief discussion on the solution to the characteristics function Eq. (22).

**Corollary 4:** The characteristics equation Eq. (22) has two distinct negative real roots for  $\varsigma \in (0, \frac{\varpi^2}{e^{-\varpi}-1})$ , has repeated real roots  $\lambda^* = \frac{e^{-\varpi}-1}{\varpi}$  for  $\varsigma = \frac{\varpi^2}{e^{-\varpi}-1}$ , has two complex roots for  $\varsigma \in (\frac{\varpi^2}{e^{-\varpi}-1}, \infty)$  in which  $\varpi = -W_0(-\frac{2}{e^2}) - 2$ .<sup>10</sup> The real part of the complex roots is negative for  $\varsigma \in (\frac{\varpi^2}{e^{-\varpi}-1}, \frac{\pi^2}{2})$ , and is positive for  $\varsigma \in (\frac{\pi^2}{2}, \infty)$ .<sup>11</sup>

*Proof:* See Appendix A.  $\square$

For  $\varsigma \in (0, \frac{\varpi^2}{e^{-\varpi}-1})$ , there are two negative real solutions, in which it holds that  $|\lambda_0| < |\lambda_1|$ . Note that  $\lambda_0$  is the dominant root. Further, we have the following approximation for the dominant root  $\lambda_0$  in the following corollary.

**Corollary 5:** It holds that  $\lambda_0 \approx \frac{2}{\varsigma-2}$  for  $\varsigma \ll 1$ .

*Proof:* By applying the second order Taylor expansion, it follows that  $\varsigma\lambda^2 \approx -\varsigma\lambda + \frac{\varsigma^2\lambda^2}{2}$ . By this means, we arrive at Corollary 5.  $\square$

#### IV. PARAMETER OPTIMIZATION FOR DISTRIBUTED SGD

In this section, we will further present run-time and staleness analysis for distributed SGD, building upon the presented theoretical performance analysis. Following this, we will reveal the protocol design criteria for distributed SGD.

##### A. Parameter Optimization for Asynchronous SGD

In this subsection, we present the probability distribution of the update interval, also referred to as the run time [14], and step staleness in  $B$ -ASGD to bridge the asynchronous SGD algorithm and the SDDE-based continuous approximation. Recall that in  $B$ -ASGD, the central server collects the first  $B$  gradients while the other clients do not halt the computation of their gradient. For the sake of discussion, we assume infinite communication bandwidth in this subsection, in which the communication delays are negligible compared to the computational delay. In this case, the gradient delay or the continuous-time gradient staleness equals the computational delay. The computational delay of each client is assumed to follow a general distribution, in which they are assumed to have a common expectation, i.e.,  $\mathbb{E}\{T_k\} = 1/\nu$ . Let  $N_p(t)$  be the aggregated arrival process of gradients to the central

<sup>10</sup>The numerical value of  $\varpi$  is  $\varpi \approx -1.5936$ . Also, it follows that  $\frac{\varpi^2}{e^{-\varpi}-1} \approx 0.6476$  and  $\lambda^* \approx -2.4608$ .

<sup>11</sup>Note that there is always a trivial solution  $\lambda = 0$  for Eq. (22).

server in  $B$ -ASGD. To ensure the validity of the Poisson approximation, it is assumed that  $B$  is much smaller than  $K$  in this section. Let  $Y \sim \text{Exp}(\nu)$  denote a random variable following an exponential distribution with a mean  $1/\nu$ . By [43]–[45], we have the following lemma.

**Lemma 2:** Given that the central server has collected  $i \in \{0, 1, \dots, B-1\}$  gradients since the last update of the global model,  $N_p(t)$  can be approximated as a Poisson process with rate  $(N-i)\nu$ .

In this way, we have the following theorem, which does not rely on exponentially distributed computation time.

**Theorem 2:** The update intervals in  $B$ -ASGD is given by

$$I = \sum_{i=1}^B I^{(i)}, \quad (23)$$

in which  $I^{(i)} \sim \text{Exp}((K-i+1)\nu)$  and  $\mathbb{E}\{I\} = \frac{1}{\nu} \sum_{i=K-B+1}^K \frac{1}{i}$ . Also, it holds that

$$\mathbb{E}\{I\} \approx \frac{1}{\nu} \left[ \log \frac{K}{K-B} - \frac{B}{2K(K-B)} \right]. \quad (24)$$

*Proof:* By the Poisson approximation of the aggregated arrival process, the update interval between the arrival of the  $(i-1)$ th and  $i$ th gradients is exponentially distributed with rate  $(K-i+1)\nu$  for  $i \in \{1, \dots, B\}$ . By this means, we get Eq. (23). Next, we have Eq. (24) by the Euler–Maclaurin formula.  $\square$

Next, we present the expectation of the step staleness in  $B$ -ASGD. Note that in  $B$ -ASGD, the step staleness equals  $BJ$  rather than  $J$  if the global model takes  $J$  iterations during the period that the client fetches the global model and finishes the computation. This is due to the fact in each iteration, the global model is updated based on all the  $B$  gradients.

**Theorem 3:** The expectation of the step staleness in  $B$ -ASGD without gradient dropout is given by<sup>12</sup>

$$\mathbb{E}\{\check{\tau}\} = K - B. \quad (25)$$

*Proof:* Let  $S^\kappa[J] = S^\kappa[J-1]$  if the Client  $\kappa$ 's contributes to one of the  $B$  gradients in the  $J$ th iteration of global model and  $S^\kappa[J] = S^\kappa[J-1] + B$  otherwise in which  $S^\kappa[0] = 0$ . In this way,  $S^\kappa[J]$  equals the sum of step gradients of all the gradients received by the central server from Client  $\kappa$  plus the step staleness of the current computing gradient. Let  $S[J] = \sum_{\kappa=1}^K S^\kappa[J]$ . In this way,  $S[J] = (K-B)BJ$  since  $B$  gradients arrive at the central server and the other  $K-B$  gradients' step staleness is increased by  $B$ . The total gradients received by the central server is  $BJ$  after  $J$  times global model updates. Since  $\mathbb{E}\{\check{\tau}\} = \lim_{J \rightarrow \infty} \frac{S[J]}{BJ}$ , we arrive at Eq. (25).  $\square$

It is observed that in  $B$ -ASGD, the reduction of step staleness is achieved by decreasing the update frequency. Next, we present a brief discussion on the difference between  $B$ -ASGD and  $B$ -batch ASGD. Similar to Theorem 2, the update interval follows an Erlang distribution, denoted by  $\text{Erlang}(B, \nu)$ , with mean  $B/\nu$  in  $B$ -batch ASGD. Further, following the discussion in Theorem 3, it holds that  $\mathbb{E}\{\check{\tau}\} = K-1$  in  $B$ -batch ASGD.

To further reduce the step staleness, the client could choose to stop the computation of the current gradient according to a continuous-time or discrete-time staleness threshold. Next, we first present the following discussion on  $B$ -ASGD with a continuous-time staleness threshold. In particular, we assume each client's computational delay follows an i.i.d. distribution, denoted by  $T$ . Let  $F_T(\cdot)$  be the cumulative distribution function of  $T$ . In this context, let  $p = F_T(\hat{\tau}_{th})$  be the probability

that a computation of gradient is not discarded due to timeout. Further,  $\bar{p} = 1 - p$ . Let  $\tilde{T}$  be the truncated computation time, in which  $F_{\tilde{T}}(s) = \frac{F_T(s)}{p}$  if  $s < \hat{\tau}_{th}$  and  $F_{\tilde{T}}(s) = 0$  for  $s > \hat{\tau}_{th}$ . In this case,  $\mathbb{E}\{\tilde{T}\} = \frac{1}{p} \int_{s=0}^{\hat{\tau}_{th}} s dF_T(s)$ . Next, we have the following proposition on the inter-update time of the  $B$ -ASGD with a continuous-time staleness threshold.

**Proposition 2:** In  $B$ -ASGD with a continuous time staleness threshold, the interval  $\Upsilon$  between consecutive updates of gradients from a specific client is given by  $\Upsilon = M\hat{\tau}_{th} + \tilde{T}$ , in which  $M$  is a geometric random variable with probability mass function  $\Pr\{M = m\} = p\bar{p}^m$  for  $m \in \mathbb{N}$ .

By the above proposition, we have the following corollary.

**Corollary 6:** The expectation of  $\Upsilon$  is given by

$$\mathbb{E}\{\Upsilon\} = \frac{\bar{p}}{p} \hat{\tau}_{th} + \frac{1}{p} \int_{s=0}^{\hat{\tau}_{th}} s dF_T(s). \quad (26)$$

*Proof:* By the expectation of the sum of random variables, we arrive at Eq. (26).  $\square$

Therefore, the rate of the aggregated gradient arrival process is given by  $\tilde{\nu} = \frac{K}{\mathbb{E}\{\Upsilon\}}$ . By Theorem 2, we have the following corollary.

**Corollary 7:** The update intervals in  $B$ -ASGD with a continuous time staleness threshold is given by  $I = \sum_{i=1}^B \text{Exp}((K-i+1)\tilde{\nu})$ , in which  $\tilde{\nu} = \frac{Kp}{(1-p)\hat{\tau}_{th} + \int_{s=0}^{\hat{\tau}_{th}} s dF_T(s)}$

and  $\mathbb{E}\{I\} = (\sum_{i=K-B+1}^K \frac{1}{i})/\tilde{\nu}$ .

Next, we have the following theorem for the step staleness in  $B$ -SGD with a continuous-time staleness threshold.

**Corollary 8:** The expectation of the step staleness in  $B$ -ASGD with a continuous time staleness threshold  $\hat{\tau}_{th}$  is approximately given by  $\mathbb{E}\{\check{\tau}\} \approx (K-B) \left( 1 - \frac{\bar{p}\hat{\tau}_{th}}{\bar{p}\hat{\tau}_{th} + \int_{s=0}^{\hat{\tau}_{th}} s dF_T(s) - \beta p \mathbb{E}\{\tilde{T}\}} \right)$ .<sup>13</sup>

Next, we turn our attention to  $B$ -ASGD with a discrete-time staleness threshold  $\check{\tau}_{th}$ . In particular, if the global model has been updated  $\check{\tau}_{th}$  times before a client finishes its computation of the current gradient, the client shall stop the computation of the current gradient and starts the computation of a new one. In this case, the step staleness of each gradient is no greater than  $B\check{\tau}_{th}$ . With memoryless computation time, we have the following proposition.

**Proposition 3:** Assuming i.i.d. exponential computation times across each client, the step staleness with a discrete-time staleness threshold  $\check{\tau}_{th}$  follows a truncated geometric distribution, i.e.,

$$\Pr\{\check{\tau} = mB\} = \frac{q\bar{q}^m}{1 - \bar{q}^{\check{\tau}_{th}+1}} \text{ for } \check{\tau} = 0, B, \dots, B\check{\tau}_{th} \quad (27)$$

in which  $q = B/K$ . Further,

$$\mathbb{E}\{\check{\tau}\} = \frac{B}{1 - \bar{q}^{\check{\tau}_{th}+1}} \left( \frac{\bar{q} - \bar{q}^{\check{\tau}_{th}+1}}{q} - \check{\tau}_{th} \bar{q}^{\check{\tau}_{th}+1} \right). \quad (28)$$

By Proposition 3, we have two observations. First,  $\lim_{\check{\tau}_{th} \rightarrow \infty} \mathbb{E}\{\check{\tau}\} = K-B$ , which fits with the results presented in Theorem 3. Next, by tuning the computation of the gradient in terms of gradient staleness, one could also reduce the gradient staleness.

## B. Parameter Optimization for Pure Asynchronous SGD

In this subsection, we focus on pure asynchronous SGD, or 1-ASGD, for deeper insights, in which  $B = 1$  and  $\hat{\tau}_{th} = \infty$ . Here we relax the assumption of identically distributed computation time across each client. Let  $T_\kappa$  be

<sup>12</sup>When  $B = 1$ , this theorem reduces to the pure asynchronous SGD case, which was presented by Eq. (18) in [15].

<sup>13</sup>Here,  $\beta \in (0, 1)$  is a constant introduced to offset the non-Poissonity of the global model update process.



the continuous-time random variable corresponding to the computational delay of the  $\kappa$ th worker. Further, it is assumed that  $0 < \mathbb{E}\{T_\kappa\} < \infty$ . Let  $\nu_\kappa = \frac{1}{\mathbb{E}\{T_\kappa\}}$  and  $\nu_p = \sum_{\kappa=1}^K \nu_\kappa$ . The sequence of the computational delay from Worker  $\kappa$  is denoted by  $(T_\kappa^{(i)})_{i \geq 1}$ . The update time of each worker can therefore be denoted by  $J_\kappa^{(n)} = \sum_{i=1}^n T_\kappa^{(i)}$ . Let us define the following stochastic process  $N_p^\kappa(t) = \sum_{n=1}^\infty \mathbb{1}\{J_\kappa^{(n)} \leq t\}$  representing the number of updates from Worker  $\kappa$  by time  $t$ . Furthermore, the rate of  $N_p^\kappa(t)$  is  $\nu_\kappa$ . In this context, the number of arrived gradients at the parameter server is given by the superposition of  $N_p^\kappa(t)$  for  $\kappa = 1, 2, \dots, K$ . More specifically, we have

$$N_p(t) = \sum_{\kappa=1}^K N_p^\kappa(t). \quad (29)$$

From Theorem 2, we have the following corollary.

**Corollary 9:** If  $N_p^\kappa(t)$  are mutually independent,<sup>14</sup>  $N_p(t)$  can be approximated as a Poisson process, the rate of which is given by  $\nu_p = \sum_{\kappa=1}^K \nu_\kappa$ .

From Theorem 3, we directly have the following corollary.

**Corollary 10:** In pure asynchronous SGD, it holds that  $\mathbb{E}\{\check{\tau}\} = K - 1$ .

First, we aim to present the distribution of the gradient staleness and the optimal choice for the number of users in pure asynchronous SGD. Let  $Y \sim \text{Pois}(\nu)$  be the random variable distributed according to a Poisson distribution with rate  $\nu$ . In this context, we have the following proposition.

**Proposition 4:** In pure asynchronous SGD, the discrete-time gradient staleness for Client  $\kappa$ 's gradient follows a mixed Poisson distribution, i.e.,

$$\check{\tau}_\kappa \sim \text{Pois}((\nu_p - \nu_\kappa)T_\kappa). \quad (30)$$

In this way, it holds that  $\mathbb{E}\{\check{\tau}_\kappa\} = (\nu_p - \nu_\kappa)/\nu_\kappa$ , and  $\text{Var}\{\check{\tau}_\kappa\} = (\nu_p - \nu_\kappa)/\nu_\kappa + (\nu_p - \nu_\kappa)^2 \sigma_\kappa^2$ , in which  $\text{Var}\{T_\kappa\} = \sigma_\kappa^2$ .

*Proof:* From the perspective of Worker  $\kappa$ , the superposition of the arrival gradients from all other workers can be modeled as a Poisson process with rate  $\nu_p - \nu_\kappa$ . By this means, we arrive at Eq. (30).  $\square$

Next, the discrete-time staleness is a mixed Poisson distribution with the rate parameter distributed according to an exponential distribution. Therefore, we have the following corollary.

**Corollary 11:** Given  $T_\kappa \sim \text{Exp}(\nu)$ , the gradient staleness in asynchronous SGD with ideal communication channel follows a geometric distribution, i.e.,  $\check{\tau}_\kappa \sim \text{Geo}\left(\frac{1}{K-1}\right)$ , in which  $K$  is the total number of workers. Further, we have  $\mathbb{E}\{\check{\tau}_\kappa\} = K - 1$  and  $\text{Var}\{\check{\tau}_\kappa\} = K(K - 1)$ .

This corollary aligns with Theorem 3 when  $B = 1$ . Further, the impact of the increase in the number of clients on the convergence of SGD is twofold. On the one hand, there is a higher volume of gradient data arriving within a given time duration. On the other hand, the increase in the number of clients can lead to a greater gradient staleness.

### C. Optimal Worker Numbers in Asynchronous SGD Through an Ideal Data Link or Network

In this subsection, our objective is to determine the optimal choice of the number of workers in asynchronous SGD with a quadratic objective function  $f(x) = \frac{1}{2}vx^2$ , assuming an ideal data link. Here, an ideal data link refers to one that is error-free and zero-delay. In pure asynchronous SGD, the expectation of

the step staleness is  $\mathbb{E}\{\check{\tau}\} = K - 1$ . Based on this fact, we present the following proposition.

**Proposition 5:** For pure asynchronous SGD through an ideal channel with a fixed learning rate, the optimal number of workers, denoted by  $K^*$ , is approximately given by

$$K^* \approx 1 + \frac{1}{v\eta e}. \quad (31)$$

*Proof:* Given the learning rate  $\eta$ , the two roots of the characteristics function can be determined by Proposition 2. Notice that it holds that  $\text{Real}(\lambda_0) < \text{Real}(\lambda_1)$  when  $\check{\tau}\eta v < \frac{1}{e}$ , and  $\text{Real}(\lambda_0) = \text{Real}(\lambda_1)$  when  $\check{\tau}\eta v \geq \frac{1}{e}$ . In this way, the convergence rate of the SGD algorithm is mainly determined by the dominant root  $\text{Real}(\lambda_0)$ , i.e.,  $\mathbb{E}\{\hat{x}(t)\} \approx \hat{x}(0)e^{\lambda_0 K \nu t}$ , in which  $\lambda_0 = \frac{W_0(-(K-1)v\eta)}{(K-1)\eta}$ . Such,  $K^* = \arg \min_K \frac{K \text{Real}(W_0(-(K-1)v\eta))}{(K-1)\eta}$ . Since  $\text{Real}\{W_0(s)\}$  achieves its minimum at  $s = -\frac{1}{e}$ , we arrive at the proposition.  $\square$

*Remark:* In this discussion, we aim to explore the effect of the number of workers on the convergence rate with a worker number-aware step size in pure asynchronous SGD. Note that the expectation of the discrete-time gradient staleness is approximately given by  $\mathbb{E}\{\check{\tau}\} \approx K$  in which  $K$  is the number of workers. In this case, we set  $\eta = \eta_0/K$  for some constant  $\eta_0$ . The dominant characteristic root is given by  $\lambda = W_0(-\eta_0 v)/\eta_0$ . Also, the update frequency is  $\nu = \frac{K}{\mathbb{E}\{\check{\tau}\}}$ . Therefore, the elapsed time in SDDE is  $\eta \nu t = \frac{\eta_0 t}{\mathbb{E}\{\check{\tau}\}}$ . Therefore, the SGD evolves according to  $\mathbb{E}\{\hat{x}(t)\} \approx \hat{x}(0) \exp \frac{W_0(-\eta_0 v)t}{\mathbb{E}\{\check{\tau}\}}$ . Therefore, it is seen that increasing  $K$  does not effectively increase the performance in asynchronous SGD with a staleness-aware step size.

Also, given the learning rate  $\eta$  and the total number of workers  $K$ , it can be seen that when  $K \geq 1 + \frac{1}{v\eta e}$  the performance of pure asynchronous SGD deteriorates due to the large step staleness. In this case, one could improve the performance by setting an appropriate  $B$ . A sensible choice of  $B$  can be  $B^* \approx K - \frac{1}{v\eta e}$  by Theorem 3.

### D. Optimal Worker Number in Pure Asynchronous SGD Through a Bandwidth Constrained Channel Shared by Multiple Workers

In this subsection, we aim to determine the optimal number of workers in pure asynchronous SGD operating through a shared medium with limited bandwidth. In this case, the continuous-time gradient staleness is characterized by the sum of the computational delay and the communication delay. In this scenario, an increase in  $K$  not only results in more frequent updates but also leads to a rise in the overall gradient delay due to increased communication delay.

Specifically, we assume a constant service time for the communication channel, given that the arriving data packets are approximately uniform in size. Still, it holds that  $\mathbb{E}\{T_\kappa\} = \frac{1}{\nu}$ ,  $\text{Var}\{T_\kappa\} = \sigma_\kappa^2$ . The service rate of the communication channel is denoted by  $\mu_Q$ . In this way, the service time for each data packet is a deterministic time  $T_Q = \frac{1}{\mu_Q}$  seconds. As per Lemma 9, the arrival process of gradients to the communication channel can be approximated as a Poisson process with rate  $\nu_p = K\nu$ . Therefore, the communication channel can be modeled as a  $M/D/1$  queue. Note that  $\nu_p$  is the rate of  $N_p(t)$ . In this way, the utility of the  $M/D/1$  queue can be denoted by  $\rho = \frac{\nu_p}{\mu_Q}$  in which  $\rho < 1$ . Therefore, the average waiting time of the gradients in the queue is given by  $W = \frac{1}{\mu_Q} \frac{\rho}{2(1-\rho)}$ .

Further, the average communication delay, which is given by the sum of the average waiting time in the queue plus the

<sup>14</sup>Note that  $N_p^\kappa(t)$  does not have to be a Poisson process. Also, by assuming that the computational delays of each worker are independent random variables, the arrival processes  $N_p^\kappa(t)$  are also mutually independent renewal processes.

average service time, is  $\mathbb{E}\{D\} = \frac{1}{\mu_Q} \left( \frac{\rho}{2(1-\rho)} + 1 \right)$ . In this way, the expectation of the continuous-time gradient staleness is given by the sum of the expectation of the computation and communication delay. More specifically, we have  $\mathbb{E}\{\hat{\tau}\} = \frac{1}{\nu} + \frac{1}{\mu_Q} \left( \frac{\rho}{2(1-\rho)} + 1 \right)$ . With limited bandwidth, the client can choose to start the computation of a new gradient right away after it finishes the computation of the previous one. It can also start the computation of the new gradient after it receives an ACK (acknowledgment) that the global model has been updated according to the gradient, which reduces the gradient staleness but also reduces the update frequency. In the latter situation, it still holds that  $\mathbb{E}\{\hat{\tau}\} = K - 1$ . In the subsequent, we focus on the former situation and we have the following proposition.

**Proposition 6:** With  $K$  workers in total, the expectation of step staleness in asynchronous SGD through a channel with a fixed service rate is approximately given by<sup>15</sup>

$$\mathbb{E}\{\check{\tau}_Q(K)\} \approx K \left( 1 + \frac{\nu}{2\mu_Q} \left( \frac{K\nu}{\mu_Q - K\nu} + 2 \right) \right), \quad (32)$$

in which  $\mu_Q$  is the service rate of the communication channel. Therefore, starting a computation of a new gradient without waiting for an ACK increases the average step staleness with a bandwidth limited channel. By Eq. (32), we present the following remark.

*Remark:* The impacts of  $K$  on the gradient staleness  $\mathbb{E}\{\check{\tau}_Q(K)\}$  are twofold. First, the increase of  $K$  lead to an increase of the communication delay, as indicated by the term  $\frac{\nu}{2\mu_Q} \left( \frac{K\nu}{\mu_Q - K\nu} + 2 \right)$  on the right-hand side of Eq. (32). Further, for a specific worker, as  $K$  increases, more gradients from other workers arrive within a given period of time, leading to a linear increase with respect to  $K$  in staleness, as indicated by the term  $K$  on the right-hand side of Eq. (32). Note that  $\mathbb{E}\{\check{\tau}_Q(K)\}$  is monotonically increasing with respect to  $K$ .

Next, we have the following proposition on the optimal number of workers in pure asynchronous SGD,

**Proposition 7:** Given the learning rate  $\eta$  and the queue capacity  $\check{K}$ , the optimal number of workers in pure asynchronous SGD can be determined as the smaller solution to the following quadratic equation:

$$\left( 1 + \frac{1}{2\check{K}} \right) x^2 - \left( 1 + \check{K} + \frac{1}{\eta\nu} \right) x + \frac{\check{K}}{\eta\nu} = 0, \quad (33)$$

in which the capacity of the queue is  $\check{K} = \frac{\mu_Q}{\nu}$ .

*Proof:* See Appendix B.  $\square$

In practice, the workers can reduce the computation time by reducing the size of the minibatch, thus increasing the frequency of gradient updates. However, this approach can lead to significant bandwidth consumption and network congestion, consequently degrading algorithm performance. Moreover, a high-resolution quantization of the gradients with large gradient noise also leads to substantial bandwidth usage, thus being inefficient due to the waste of network bandwidth.

### E. Optimal Design for Event-Triggered Distributed Optimization

In this subsection, we present a discussion on distributed learning with event-triggered communication, which is presented in the literature to effectively save the bandwidth [23].

Given the state variable at  $t_0$ , denoted by  $\mathbf{x}_0$ , the determination of the triggering time can be formulated as the first

exit time of a continuous-time stochastic process (4), i.e.,  $H_E = \inf\{t \geq t_0 | \mathbf{x}(t) \in E(\mathbf{x}_0), \mathbf{x}(t_0) = \mathbf{x}_0\}$ , in which  $E(\mathbf{x}) = \{\mathbf{x} | \|\nabla f(\mathbf{x}) - \nabla f(\mathbf{x}_0)\| \geq \xi\}$ . Following the discussion in Subsection III-B, we assume that the triggering time is a Gaussian random variable, i.e.,  $H_E \sim \mathcal{N}(\vartheta, \zeta^2)$ . In this case, gradient staleness also arises in event-triggered SGD. Given  $H_E = \zeta$ , the conditional gradient staleness approximately follows a uniform distribution  $U(0, \zeta)$ . Therefore, the gradient staleness follows a compound distribution, i.e.,  $\tau \sim U(0, H_E)$ . Further, it is assumed that  $\vartheta \gg \zeta$ . By the law of total expectation, it holds that  $\mathbb{E}\{\tau\} = \frac{\vartheta}{2}$ . Further, the p.d.f. of  $\tau$  is given by  $p_\tau(s) = \int_s^\infty \frac{1}{\sqrt{2\pi\zeta s}} e^{-\frac{1}{2}(\frac{s-\vartheta}{\zeta})^2} ds$ , for  $s \geq 0$ . In this case, approximately uniformly distributed gradient staleness arises distributed SGD in with ETC when  $\vartheta \gg \zeta$ . Next, for the solvable case, i.e., with the quadratic objective function  $f(\mathbf{x}) = \frac{1}{2}\mathbf{x}^T \mathbf{V} \mathbf{x}$ , the expectation of the triggering-time in event-triggered SGD is approximately given by  $\mathbb{E}\{H_E\} \approx \xi \sqrt{\frac{1}{\mathbf{x}_0^T \mathbf{V}^4 \mathbf{x}_0}}$  when  $\xi \ll \|\mathbf{x}_0\|_2$ . Note that different from the previous discussion, SGD along different eigenvector directions can not be viewed as independent in event-triggered SGD.

In distributed learning with event-triggered communication, the step staleness is  $\check{\tau} = \hat{\tau}/T_s$  in which  $T_s$  is the timeslot duration in event-triggered SGD. In addition, we have  $\tau = \eta\hat{\tau}/T_s$ . Next, we focus on the optimal number of workers in event-triggered SGD given the total bandwidth constraint, in which we limit our discussion to the one-dimensional solvable objective function in which  $v = 1$ .

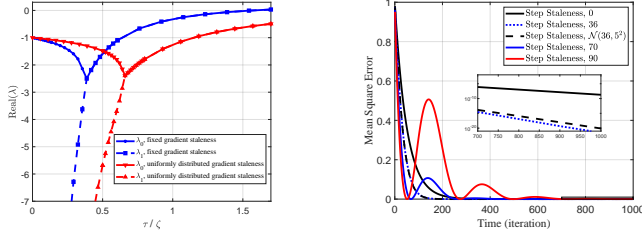
*Remark:* Let  $C$  be the total bandwidth allocated to the uplink channel in event-triggered SGD. More specifically, the workers can update up to  $C$  gradients to the parameter server per second on average. We assume that the triggering threshold is carefully chosen such that the communication channel is fully utilized and the workers are assumed to be homogeneous. Recall that the expectation of the triggering-time is denoted by  $\mathbb{E}\{H_E\} = \vartheta$ . In this way, the gradient staleness in SDDE is approximately uniformly distributed, i.e.,  $\tau \sim U(0, \vartheta)$ , in which  $\vartheta = \frac{K\eta}{CT_s}$ . Note that  $\eta$  is the fixed learning rate and  $T_s$  is the time slot length in distributed learning with event-triggered communication. Similar to the discussion in Subsection IV-D, the optimal number of workers is approximately the number of workers at which the gradient staleness minimizes the real part of the dominant root. In this way, we conclude that the optimal number of workers is approximately given by  $K^* = \frac{C\varpi^2 T_s}{\eta(e^{-\varpi} - 1)}$  given a total bandwidth constraint in distributed learning with event-triggered communication. Given a total bandwidth limit, too many workers can induce a large degree of gradient staleness and the performance of event-triggered SGD can therefore deteriorate.

## V. NUMERICAL RESULTS

In this section, we shall present simulation and numerical results to verify the theoretical analysis for distributed SGD with stale gradient. We will further demonstrate the effect of gradient noise, step size, and gradient staleness on asynchronous SGD.

To illustrate the relationship between the roots of the characteristic function and the gradient staleness, Fig. 2(a) presents numerical results for the characteristic roots of Eq. (16) and Eq. (22). In particular, we consider a fixed gradient staleness, denoted by  $\tau$ , or a uniformly distributed gradient staleness, denoted by  $\tau \sim \text{Uni}(0, \zeta)$ , respectively. In both cases, the real part of the dominant root first decreases, then increases as  $\tau$  or  $\xi$  increases. With a fixed gradient staleness, the real part of the root achieves its minimum, i.e.,  $\text{Real}(\lambda_0) = -e$  when  $\tau = 1/e$ , while for uniformly distributed gradient staleness, the real part of the root achieves its minimum when  $\zeta = 0.6476$ .

<sup>15</sup>The arrival process of the gradients to the central server is the departure process of the  $M/D/1$  queue. Rigorously, the departure process of the  $M/D/1$  is not a Poisson process. But the intensity of the departure process equals the intensity of the arrival process to the queue as long as  $\mu_Q > \nu$ .



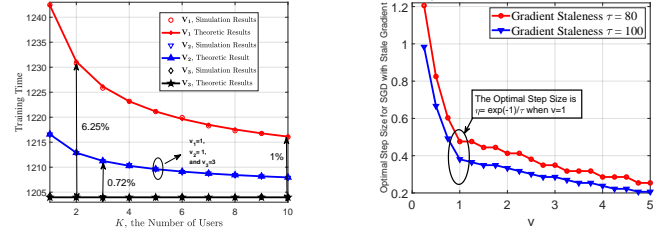
(a) The roots of the characteristic functions. (b) The relationship between the convergence rate and the gradient staleness for the solvable cases.

Fig. 2. The impact of  $\tau$  on the convergence of the SGD algorithm.

The above results demonstrate that an SGD algorithm achieves performance gain with an appropriate gradient staleness. This may be counterintuitive that the gradient staleness does not always impede the convergence of the SGD method. However, the SGD process oscillates when  $\tau > 1/e$  or  $\zeta$ , and diverges when  $\tau > \frac{\pi}{2}$  or  $\zeta > \frac{\pi}{2}$ . This illustrates that the convergence property considerably deteriorates with large a gradient staleness. To validate the aforementioned discussion on the roots of the characteristic function, Fig. 2(b) presents the effect of gradient staleness on the convergence rate of SGD with gradient staleness. To avoid the impact of gradient noise on SGD, we set  $\sigma = 0$ . Also, the learning rate is  $\eta = 0.01$ , and we adopt the same objective function as in Fig. 2(a). We observe that, as the discrete-time gradient staleness increases from 0 to 36, an increased degree of gradient staleness leads to faster convergence. While as the gradient staleness further increases, i.e., when  $\eta\tilde{\tau} > 1/e$ , SGD oscillates, which leads to slower converges. Further, it can be seen that when  $\tilde{\tau} \sim N(36, 5^2)$ , SGD nearly has the nearly same converges rate as when the discrete-time gradient staleness is a constant given by  $\mathbb{E}\{\tilde{\tau}\}$ .

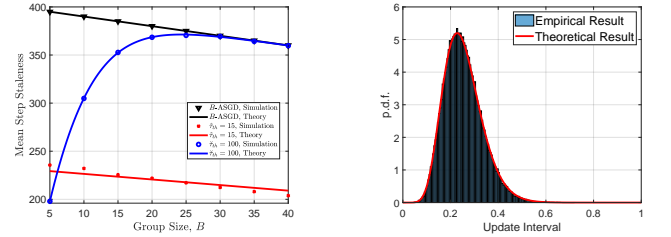
To reveal the optimal choice of the learning rate in multi-dimensional optimization, Fig. 3(b) is presented. In particular,  $f(\mathbf{x}) = \frac{1}{2}\mathbf{x}^T\mathbf{V}\mathbf{x}$  in which  $\mathbf{V} = \text{diag}(v, 1)$ . Notably,  $\|\mathbf{V}\|_2 = \max\{v, 1\}$ . Given the discrete-time gradient staleness and  $v$ , we numerically find the optimal (fixed) step size, i.e., the step-size that leads to the minimum loss after  $1 \times 10^5$  iterations, by exhaustive search. For example, it is seen that  $\eta^* = \frac{1}{e\tilde{\tau}}$  when  $v = 1$ , which agrees with Eq. (18). Notably, we observe that it always holds that  $\eta^* \in [1/(e\|\mathbf{V}\|_2), \pi/(2\|\mathbf{V}\|_2)]$ , which is consistent with Eq. (19) in Subsection III-C. This is due to the fact that, when  $\eta > \pi/(2\|\mathbf{V}\|_2)$ , in the eigenvector direction which the largest eigenvalue, SGD diverges. While SGD converges slower along each eigenvector direction by further reducing the learning rate when  $\eta < 1/(e\|\mathbf{V}\|_2)$ .

In the subsequent, we verify our differential equation-based performance analysis on the effect of the gradient noise in Fig. 3(a). To avoid the impact of gradient staleness on the convergence of SGD, we study  $K$ -synchronized SGD. The objective functions are  $f_i(\mathbf{x}) = \frac{1}{2}\mathbf{x}^T\mathbf{V}_i\mathbf{x}$ , in which  $\mathbf{V}_1 = \text{diag}(1, 1, 1)$ ,  $\mathbf{V}_2 = \text{diag}(1, 1, 3)$ , and  $\mathbf{V}_3 = \text{diag}(1, 2, 3)$ . Also, the variance of the additive Gaussian noise is inversely proportional to the square root of  $K$ , in which  $K$  is the number of workers. It is seen that in quadratic optimization, the number of iterations for an SGD algorithm is mainly determined by the smallest eigenvalue. Further, it can be observed that the average iterations for the SGD algorithm to meet the stopping criterion stays nearly unchanged despite the increases in the number of users with the objective function  $f_3(\mathbf{x})$ . This is due to the fact that the average first hitting time of a one-dimensional OU-process remains unchanged with respect to the variance of the additive Gaussian noise



(a) Number of iterations required for synchronous SGD with  $K$  workers to converge. (b) The optimal learning rate for asynchronous SGD.

Fig. 3. The impact of the gradient noise and the choice of learning rate.



(a) Step staleness in  $B$ -ASGD. (b) The probability distribution of the update interval in  $B$ -ASGD.

Fig. 4. Run-time and step staleness in  $B$ -ASGD.

as suggested by Lemma 1. Further, it is seen that the training time slightly decreases with the increase of  $K$  with  $\mathbf{V}_1$ , which fits well with Eq. (13). This is due to the fact the decrease in the noise variance leads to a decrease in the variance of the first hitting times along each eigenvector. In addition, we observe that, the differential-equation based approach presents an accurate performance analysis with a quadratic function. Also, it should be noted that the increase of  $K$  reduces the variance of the training time.

Next, we aim to verify the presented run-time and step staleness analysis for  $B$ -ASGD. Fig. 4(a) presents the expectation of the step staleness versus  $B$  in  $B$ -ASGD. In particular, we have  $K = 400$ , in which  $T \sim \mathcal{N}(10, 3^2)$  for  $B$ -ASGD,  $T \sim U(0, 20)$  for  $B$ -ASGD with a continuous-time gradient staleness threshold  $\hat{\tau}_{th} = 15$ , and  $T \sim \text{Exp}(1/10)$  for  $B$ -ASGD with a discrete-time gradient-staleness  $\tilde{\tau} = 100$ . It is observed that the numerical results fit well with the theoretical results, which verifies our discussions in Subsection IV-A. Further, Fig. 4(b) presents the update interval of  $B$ -ASGD in which  $K = 400$ ,  $B = 10$ , and  $T \sim \mathcal{N}(10, 3^2)$ . It is seen the empirical results fit well with the theoretical results, which verifies Theorem 2 and the Poisson approximation of the aggregated gradient arrival process, even with non-exponentially distributed computation time.

In the following simulations, we investigate the effect of gradient noise and staleness and verify our performance analysis based on empirical results on the MNIST handwritten digit database. First, we present the effect of the number of users on asynchronous learning with a fixed learning rate. In particular, the learning rate is  $\eta = 0.01$ . The computational delay of each worker follows an i.i.d. Gaussian distribution  $\mathcal{N}(10, 1^2)$  and the communication delay is assumed to be negligible.

Fig. 5(a) presents the performance of asynchronous learning with respect to wall-clock time on the MNIST dataset with a convolutional neural network (CNN). First, similar to the solvable cases, the performance of asynchronous learning first



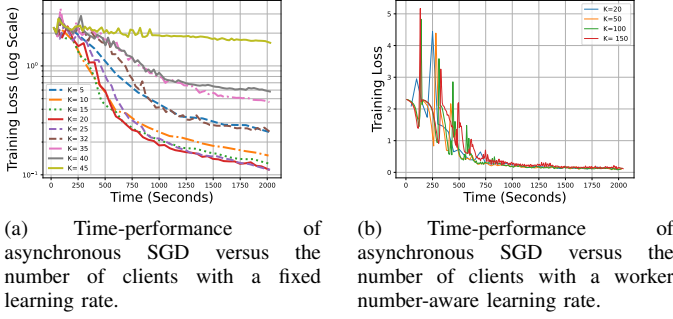


Fig. 5. Asynchronous SGD with gradient staleness on the MNIST dataset.

increases with the increase of  $K$  (or step staleness), then decreases. It is seen that when there are fewer workers, for example,  $K = 5$ , asynchronous SGD converges slowly. This is due to the fact that with small  $K$ , the number of gradients collected by the global model is also limited. Further, when  $K = 20$ , the asynchronous SGD algorithm achieves nearly the best performance. Another observation that can be made from Fig. 5(a) is that when  $K \geq 20$ , the performance of asynchronous SGD deteriorates, which diverges when  $K \geq 40$ . The reason for this is that gradients staleness becomes significant as  $K$  increases, which leads to the divergence of asynchronous SGD. Note that the discrete-time gradient staleness is of significance in our analysis, which is defined as the number of global model updates between two consecutive gradient updates for the same user. This is different from the continuous-time gradient staleness with respect to the wall-clock time. These results demonstrate that, too many workers in asynchronous learning can considerably deteriorate the efficiency of the algorithms.<sup>16</sup>

With a fixed step-size, the performance of asynchronous SGD is shown to deteriorate with a large number of workers, or equivalently, with a large degree of gradient staleness. Next, we aim to evaluate the performance of asynchronous SGD with a worker number-aware step-size. In particular, we adopt the same setup as the experiment presented in Fig. 5(a). Fig. 5(b) presents the performance of asynchronous SGD with worker number-aware step size. In particular, the step size is  $\eta(K) = \frac{\eta_0}{K}$ , wherein  $K$  is the number of workers and  $\eta_0 = 0.2$  is a constant. In this case, it is seen that the asynchronous SGD algorithm converges with a worker number-aware step size. However, a careful reader may also notice that the performance of the SGD algorithm does not significantly improve with the increase of  $K$  in terms of wall-clock time. This is due to the fact that the positive effect of the increased number of gradients as  $K$  increases is offset by the step size inversely proportional to the number of users. While asynchronous learning can outperform synchronous learning with respect to the wall-clock time with a relatively small  $K$ . This observation aligns with the literature, such as [14].

<sup>16</sup>In the simulation, we have also presented a rough estimation of the norm-2 of the Hessian matrix  $\mathbf{H}$  of the employed CNN, which indicates that  $\|\mathbf{H}\|_2$  falls in the interval  $(3, 5)$  during the first several iterations. When  $K = 20$ , asynchronous SGD almost achieves the optimal performance. In this case, we have  $\mathbb{E}\{\tilde{\tau}\} \approx 20$ . Hence, we have  $\eta\mathbb{E}\{\tilde{\tau}\}\|\mathbf{H}\|_2 \in (0.6, 1.0)$ . Note that, for the solvable cases, a necessary condition for asynchronous SGD to achieve optimal performance is  $\eta\mathbb{E}\{\tilde{\tau}\}\|\mathbf{H}\|_2 \in (1/e, \pi/2)$ . Also, asynchronous SGD diverges when  $\mathbb{E}\{\tilde{\tau}\} \geq 40$ , which agrees with the argument in Eq. (19) for solvable cases in which asynchronous SGD diverges when  $\eta\mathbb{E}\{\tilde{\tau}\}\|\mathbf{H}\|_2 > \pi/2$ . This suggests the potential that the results for the solvable cases can be extended to general non-convex cases.

## VI. CONCLUSION

In this work, we have presented performance analysis and protocol design criteria for distributed SGD with gradient staleness through an SDDE-based approach. To deal with non-exponentially distributed computation time, a Poisson approximation for the superposition of independent renewal processes has been adopted, based on which we have presented the run-time and staleness analysis of asynchronous SGD. In this way, we have bridged the behavior of the asynchronous SGD algorithm with gradient staleness and the solution of certain SDDE. We have derived the convergence condition of distributed SGD by analyzing its characteristic roots, which allows us to optimize scheduling policies for asynchronous distributed SGD. In particular, the characteristic roots have been shown to be closely related to the learning rate, step staleness, and the eigenvalues of the objective function's Hessian matrix. It has been shown that the presence of a small gradient could slightly accelerate the convergence of the SGD, while a large degree of gradient staleness leads to its convergence. It has also been shown that, regardless of the specific distribution of computation time, the expectation of the step staleness in asynchronous SGD without gradient dropout is determined only by the number of workers and the group size. With limited bandwidth, excessive workers can lead to a large communication delay due to network congestion, degrading the performance of SGD. Further, we have also extended the derivation of the characteristic roots of the case where the gradient staleness in SDDE follows a uniform distribution, which arises in event-triggered SGD. In practice, for a given learning rate, it has been shown that there exists an optimal number of workers in the asynchronous SGD tasks, for the fact that a large number of workers leads to a greater degree of staleness which may lead to divergence of the SGD algorithm. Numerical simulation results have been presented to demonstrate the potential of our SDDE framework, even in complex learning tasks with non-convex objective functions.

It is noteworthy that the step staleness or discrete-time staleness, rather than the gradient delay, plays a crucial role in determining the convergence rate of asynchronous SGD. While asynchronous learning has been demonstrated to outperform synchronous learning with respect to the wall-clock time with a small number of users, the performance of asynchronous learning does not significantly improve with additional workers, mainly due to the enlarged gradient staleness. In this paper, we have mainly focused on the solvable cases, but we have also provided quite suggestive and analytical discussion. Important potential directions for extending our works involve extending the analytical SDDE-based framework of asynchronous SGD with gradient staleness to nonconvex objective function, and performance analysis of asynchronous SGD with a staleness-aware learning rate or involving a wireless channel.

## APPENDIX A PROOF OF COROLLARY 4

Let  $\omega = \zeta\lambda$ . It holds that  $\zeta = \frac{\omega^2}{e^{-\omega}-1}$  by Eq. (22). Let us define  $g(\omega) = \frac{\omega^2}{e^{-\omega}-1}$ . Therefore, the derivative of  $g(\omega)$  with respect to  $\omega$  is given by  $g'(\omega) = \frac{2\omega(e^{-\omega}-1) + \omega^2 e^{-\omega}}{(e^{-\omega}-1)^2}$ . Therefore,  $g(\omega)$  is monotonically increasing in  $(-\infty, \varpi)$  and monotonically decreasing in  $(\varpi, \infty)$  in which  $g'(\varpi) = 0$ . Further, it holds that  $(\varpi + 2)e^{-(\varpi+2)} = 2e^{-2}$ . Hence, we have  $\varpi = -W_0(-\frac{2}{e^2}) - 2$ . Therefore, the characteristics equation Eq. (22) has two distinct negative real roots for  $\zeta \in (0, \frac{\varpi^2}{e^{-\varpi}-1})$ . Further, suppose the solution for Eq. (21) is pure imaginary when  $\omega = \gamma$ , i.e.,  $\lambda = i\theta$ . In this case, it holds that  $\sin(-\gamma\theta) = 0$  and  $\cos(-\gamma\theta) = -\gamma\theta^2 + 1$ . Therefore,

we have  $\gamma = \frac{\pi^2}{2}$  and  $\theta = \pm \frac{2}{\pi}$ . By this means, we arrive at Corollary 4.

## APPENDIX B PROOF OF PROPOSITION 7

By modeling the communication channel with a fixed service rate in pure asynchronous SGD as an  $M/D/1$  queue, the convergence rate of the asynchronous SGD algorithm is given by  $\lambda_Q \approx \frac{W_0(-\mathbb{E}\{\tau_Q\}\eta\nu)}{\mathbb{E}\{\tau_Q\}\eta}$ , in which  $\mathbb{E}\{\tau_Q\}$  is given by Eq. (32). Therefore, the optimum number of workers in asynchronous SGD through a queue can be determined by solving the following optimization problem  $\min_{K \leq K_{\max}} \frac{\text{Real}\{W_0(-K\eta\nu z(K))\}}{\eta z(K)}$ , in which  $\tilde{K} = \frac{\mu_Q}{\nu}$  is the capacity of the queue and  $z(K) = 1 + \frac{1}{2K} \left( \frac{K}{K-K} + 2 \right)$ . Next, the optimal number of workers in this setting, denoted by  $K_Q^*$ , should satisfy that  $0 < K_Q^* \eta \nu z(K_Q^*) \leq \frac{1}{e}$  such that the  $W_0(-K_Q^* \eta \nu z(K_Q^*))$  is real since  $z(K)$  is monotonically increasing with  $K$ . Therefore, we could focus on the following optimization problem:

$$\min_{0 < K z(K) \leq \frac{1}{e\eta\nu}} \frac{W_0(-K\eta\nu z(K))}{z(K)}. \quad (34)$$

By calculating the first derivative of (34), we conclude that the optimum solution to (34) can be determined by solving  $\frac{K z'(K)}{z(K) + K z'(K)} = \frac{1}{1 + W_0(-K\eta\nu z(K))}$ , in which  $z'(K) = \frac{\tilde{K}}{(K-K)^2}$ . Since  $W_0(s)$  achieves its minimum  $W_0(s) = -1$  at  $s = 1/e$ , the optimal solution  $K_Q^*$  approximately satisfies  $K_Q^* \eta \nu z(K_Q^*) = \frac{1}{e}$ . By this means, we arrive at Eq. (33).

## REFERENCES

- [1] K. B. Letaief, W. Chen, Y. Shi, J. Zhang, and Y. A. Zhang, "The roadmap to 6G: AI empowered wireless networks," *IEEE Commun. Mag.*, vol. 57, no. 8, pp. 84-90, Aug. 2019.
- [2] D. Foley and J. Danskin, "Ultra-performance pascal GPU and NVLink interconnect," *IEEE Micro.*, no. 2, pp. 7-17, Apr. 2017.
- [3] D. Bertsekas and R. Gallager, *Data Networks*. Englewood Cliffs, NJ: Prentice-Hall, 1988.
- [4] L. Dai and X. Sun, "A unified analysis of IEEE 802.11 DCF networks: Stability, throughput and delay," *IEEE Trans. Mobile Computing*, vol. 12, no. 8, pp. 1558-1572, 2013.
- [5] J. F. Kurose and K. W. Ross, *Computer Networking - A Top-Down Approach Featuring the Internet*, 7th ed. Addison-Wesley Professional, 2012.
- [6] S. Yu, W. Chen, and H. Vincent Poor, "Distributed stochastic optimization with random communication and computational delays: Optimal policies and performance analysis," in *IEEE Proc. Int. Conf. Commun. (ICC)*, Denver, CO, Jun. 2024.
- [7] J. Chen, X. Pan, R. Monga, S. Bengio, and R. Jozefowicz, "Revisiting distributed synchronous SGD," 2016. [Online]. Available: arXiv:1604.00981.
- [8] R. Leblond, F. Pedregosa, and S. Lacoste-Julien, "ASAGA: Asynchronous parallel saga," in *Proc. Int. Conf. Artif. Intell. Statist. (AISTATS)*, 2017, pp. 46-54.
- [9] M. Li et al., "Scaling distributed machine learning with the parameter server," in *Proc. USENIX Symp. Oper. Syst. Design Implement.*, Oct. 2014, pp. 583-598.
- [10] B. Woodworth, K. K. Patel, S. Stich, Z. Dai, B. Bullins, B. McMahan, O. Shamir, and N. Srebro, "Is local SGD better than minibatch SGD?" in *Proc. Int. Conf. Mach. Learn. (ICML)*, pp. 10334-10343, 2020.
- [11] A. Odena, "Faster asynchronous SGD," 2016. [Online]. Available: arXiv:1601.04033, pp. 1-7, July 2016.
- [12] S. Yu, W. Chen, and H. V. Poor, "Real-time monitoring with timing side information," *IEEE Trans. Commun.*, vol. 71, no. 4, pp. 1953-1969, 2023.
- [13] S. Yu, W. Chen, and H. Vincent Poor, "Real-time monitoring of chaotic systems with known dynamical equations," *IEEE Trans. Signal Process.*, vol. 72, pp. 1251-1268, 2024.
- [14] S. Dutta, J. Wang, and G. Joshi, "Slow and stale gradients can win the race," *IEEE J. Sel. Areas Info. Theory*, vol. 2, no. 3, pp. 1012-1024, 2021.
- [15] H. Al-Lawati and S. C. Draper, "Staleness analysis in asynchronous optimization," *IEEE Trans. Signal Inf. Process. Netw.*, vol. 8, pp. 404-420, 2022.
- [16] T.-H. Chang, M. Hong, W.-C. Liao and X. Wang, "Asynchronous distributed ADMM for large-scale optimization—part I: Algorithm and convergence analysis," *IEEE Trans. Signal Process.*, vol. 64, no. 12, pp. 3118-3130, June, 2016.
- [17] S. Yu, W. Chen, and H. V. Poor, "Communication-constrained distributed learning: TSI-aided asynchronous optimization with stale gradient," in *Proc. IEEE Global Commun. Conf. (GLOBECOM)*, pp. 1-6, Dec. 2023.
- [18] C. Xie, S. Koyejo, and I. Gupta, "Asynchronous federated optimization," in *Proc. 12th Annual Workshop Optim. Mach. Learn.*, Mar. 2019, pp. 2350-2356.
- [19] W. Zhang, S. Gupta, X. Lian, and J. Liu, "Staleness-aware Async-SGD for distributed deep learning," in *Proc. Int. Jt. Conf. Artif. Intell. (IJCAI)*, New York, NY, USA, pp. 1-7, July 2016.
- [20] S. Barkai, I. Hakimi and A. Schuster, "Gap-aware mitigation of gradient staleness," in *Proc. Int. Conf. Learn. Representations (ICLR)*, 2019.
- [21] S. Zheng et al., "Asynchronous stochastic gradient descent with delay compensation," in *Proc. Int. Conf. Mach. Learn. (ICML)*, pp. 4120-4129, Aug. 2017.
- [22] G. M. Lipsa and N. C. Martins, "Remote state estimation with communication costs for first-order LTI systems," *IEEE Trans. Auto. Control*, vol. 56, no. 9, pp. 2013-2025, Sept. 2011.
- [23] X. He, X. Yi, Y. Zhao, K. H. Johansson, and V. Gupta, "Asymptotic analysis of federated learning under event-triggered communication," *IEEE Trans. Signal Process.*, vol. 71, pp. 2654-2667, 2023.
- [24] T. Chen, G. Giannakis, T. Sun, and W. Yin, "Lag: Lazily aggregated gradient for communication-efficient distributed learning," in *Adv. Neural Inf. Process. Syst.*, Dec. 2018, pp. 5050-5060.
- [25] T. Chen, Y. Sun, and W. Yin, "Communication-adaptive stochastic gradient methods for distributed learning," *IEEE Trans. Signal Process.*, vol. 69, pp. 4637-4651, 2021.
- [26] N. Mohammadi, J. Bai, Q. Fan, Y. Song, Y. Yi, and L. Liu, "Differential privacy meets federated learning under communication constraints," *IEEE Internet Things J.*, vol. 9, no. 22, pp. 22204-22219, Nov. 2022.
- [27] D. P. Bertsekas, *Nonlinear Programming*. Cambridge, MA, USA: MIT Press, 1999.
- [28] X. Li and F. Orabona, "On the convergence of stochastic gradient descent with adaptive stepsizes," in *Proc. Int. Conf. Artif. Intell. Statist. (AISTATS)*, vol. 89, pp. 983-992, Apr. 2018.
- [29] A. Nedić and D. Bertsekas, "Incremental subgradient methods for nondifferentiable optimization," *SIAM J. Optim.*, vol. 12, no. 1, pp. 109-138, Jan. 2001.
- [30] A. Alekh and J. C. Duchi, "Distributed delayed stochastic optimization," in *Adv. Neural Inf. Process. Syst.*, pp. 873-881, Dec. 2011.
- [31] J. Wu, W. Huang, J. Huang, and T. Zhang, "Error compensated quantized SGD and its applications to large-scale distributed optimization," in *Proc. Intl. Conf. Mach. Learning (ICML)*, pp. 5321-5329, Jul. 2018.
- [32] J. N. Tsitsiklis, D. P. Bertsekas, and M. Athans, "Distributed asynchronous deterministic and stochastic gradient optimization algorithms," *IEEE Trans. Auto. Control.*, vol. 31, no. 9, pp. 803-812, 1986.
- [33] L. He, Q. Meng, W. Chen, Z. Ma, and T. Liu, "Differential equations for modeling asynchronous algorithms," in *Proc. Int. Joint Conf. Artif. Intell. (IJCAI)*, pp. 2220-2226, 2018.
- [34] Z. Zhou, P. Mertikopoulos, N. Bambos, P. Glynn, Y. Ye, L. Li, and F. Li, "Distributed asynchronous optimization with unbounded delays: How slow can you go?" in *Proc. Int. Conf. Mach. Learn. (ICML)*, pp. 5970-5979, 2018.
- [35] K. Harold and G. Yin, *Stochastic Approximation and Recursive Algorithms and Applications*. New York, NY, USA: Springer, 2003.
- [36] Z. Li, S. Malladi, and S. Arora, "On the validity of modeling sgd with stochastic differential equations (sdes)," in *Adv. Annual Conf. Neural Inf. Process. Syst.*, 2021, pp. 12712-12725.
- [37] S. Mandt, M. D. Hoffman, and D. M. Blei, "A variational analysis of stochastic gradient algorithms," in *Proc. Int. Conf. Mach. Learn. (ICML)*, pp. 354-363, Jun. 2016.
- [38] Q. Li, C. Tai, and E. Weinan, "Stochastic modified equations and adaptive stochastic gradient algorithms," in *Proc. Int. Conf. Mach. Learn. (ICML)*, vol. 70, pp. 2101-2110, July 2017.
- [39] R. Kumar, T. Venkatesh, and K. Swarup, "Stochastic delay differential equations: Analysis and simulation studies," *Chaos, Solitons & Fractals*, vol. 165, pp. 1-23, Nov. 2022.
- [40] E. Hazan, K. Y. Levy, and S. Shalev-Shwartz, "On graduated optimization for stochastic non-convex problems," in *Proc. Intl. Conf. Mach. Learning (ICML)*, 2016, pp. 1833-1841.
- [41] A. Panigrahi, R. Somani, N. Goyal, and P. Netrapalli, "Non-Gaussianity of stochastic gradient noise," 2019. [Online]. Available: arXiv:1910.09626.
- [42] A. J. Siegert, "On the first passage time probability problem," *Phys. Rev.*, vol. 81, no. 4, 1951.
- [43] D. P. Heyman and M. J. Sobel, *Stochastic Models in Operations Research, Vol. I: Stochastic Processes and Operating Characteristics*. New York: McGraw-Hill, 1982.
- [44] C. Y. T. Lam and J. P. Lehoczky, "Superposition of renewal processes," *Adv. in Appl. Probab.*, vol. 23, no. 1, pp. 64-85, 1991.
- [45] D. R. Cox and W. L. Smith, "On the superposition of renewal processes," *Biometrika*, vol. 41, no. 1-2, p. 91, 1954.
- [46] J.B. Rosen and R.F. Marcia, "Convex quadratic approximation," *Comput. Optim. Appl.* 28, pp. 173-184, 2004.
- [47] M. Powell, "Uobyq: unconstrained optimization by quadratic approximation," *Math. Program. Ser. B* 92, pp. 555-582, 2002.
- [48] C.-p. Lee and S. J. Wright, "Inexact successive quadratic approximation for regularized optimization," *Comput. Optim. Appl.*, vol. 72, no. 3, pp. 641-674, 2019.
- [49] D. Karlis and E. Xekalaki, "Mixed Poisson distributions," *Int. Statist. Rev.*, vol. 73, no. 1, pp. 35-58, 2005.
- [50] A. J. Siegert, "On the first passage time probability problem," *Phys. Rev.*, vol. 81, no. 4, 1951.
- [51] S. Guillouzic, I. L. Heuroux, and A. Longin, "Small delay approximation of stochastic delay differential equations," *Phys. Rev. E*, vol. 59, no. 4, Apr. 1999.